

Neogene palaeoenvironments and hydrocarbon potential in the Nile Delta, Egypt: Palynological evidence from an onshore well

Mennat-Allah T. El Hussieny, Magdy S. Mahmoud*, Amr S. Deaf

Geology Department, Faculty of Science, Assiut University, Assiut 71516, Egypt

Received 9 January 2025; received in revised form 17 April 2025; accepted 27 May 2025

Available online 2 June 2025

Abstract

Palynological organic matter (POM) of the Neogene succession from the Sidi Salim-1 well, located in the onshore Nile Delta, Egypt (Eastern Mediterranean), suggests a wide range of environments, from deltaic to offshore marine. These environments were discriminated by the overall palynofacies composition, including indicative dinoflagellate cysts, mainly *Spiniferites* and *Selenopemphix*. Near-shore marine environment was interpreted for the Middle Miocene (Langhian–Serravallian) Sidi Salim Formation. Deltaic to shallow marine environments were suggested for the Qawasim (Miocene) and Kafr El Sheikh (Pliocene) formations, while the distant (offshore) marine setting was established in the Pliocene Abu Madi Formation. This deeper environment, of the Abu Madi Formation, can be used to confirm a previous documentation of an Early Pliocene progressive drowning of an incised valley, related to the Messinian Salinity Crises (MSC) events, by the late Messinian sea level drop in the Mediterranean. Suboxic to anoxic conditions existed during deposition of the investigated well succession. Anoxia was confirmed by the occurrence of imprints of pyrite crystals across much of the well succession. The occurrence of abundant Poaceae pollen may suggest widespread dry grassland vegetation during deposition of the Neogene sediments of the well. In a regional context, the Neogene environments in the Nile Delta area vary according to the relative position of the investigated sediments, due to structural, palaeogeographic and basinal settings. The recovered palynofacies fluctuated between amorphous organic matter (AOM)-dominated and phytoclast-dominated categories, mostly of the kerogen type II, which is capable of producing oil and gas. The visual assessment of the spore coloration index (SCI) of thin-walled trilete spores in the well section, shows values ranging between 5 and 8, confirming a thermally mature organic matter and, consequently, can be potential source rocks. © 2025 Elsevier B.V. and Nanjing Institute of Geology and Palaeontology, CAS. All rights are reserved, including those for text and data mining, AI training, and similar technologies.

Keywords: Palynofacies; Spores-pollen; Dinoflagellate cysts; Messinian Salinity Crises (MSC); Miocene–Pliocene transition

1. Introduction

The Nile Delta is one of the best-known deltas in the world. It contains a thick sedimentary succession covering the basement rocks and is considered an important hydrocarbon producing province in Egypt, mainly from the Neogene (Miocene–Pliocene) rock units (Abu Madi, Qawasim and Kafr El Sheikh formations). Extensive research on

the geology and source-rock evaluation of the Neogene subsurface rocks in the region have been published (e.g., Rizzini et al., 1978; El Beialy, 1990a, 1990b, 1992, 1997; Abdel Aal et al., 1994, 2000; Sarhan and Hemdan, 1994; Ouda and Obaidalla, 1995; Sestini, 1995; Kamel et al., 1998; Zaghoul et al., 2001; Leila et al., 2019; Shebl et al., 2019; El-Kahawy et al., 2022; Metwalli et al., 2023; Nabawy et al., 2023; Shalaby and Sarhan, 2023; Mahmoud et al., 2024; Soliman and El Atfy, 2024 and comprehensive literature therein).

* Corresponding author.

E-mail address: magdysm@aun.edu.eg (M.S. Mahmoud).

Recently, a few palynofacies studies were incorporated in the Nile Delta area (Makled et al., 2013; El Diasty et al., 2019; El Atfy 2021; Mahmoud et al., 2024). In general, the Miocene (23.03–5.33 Ma) witnessed significant climatic and oceanographic variability. The Messinian Salinity Crises (MSC) (5.97–5.33 Ma), an enigmatic episode of palaeoceanographic change, is a matter of interest throughout the Mediterranean Basin. It is generally accepted that during the MSC interval there was a dry climate in the Mediterranean region (Vasiliev et al., 2017), which is reflected in dinoflagellate cyst assemblages, indicating an ecological turnover linked to basin desiccation and re-flooding (e.g., Clauzon et al., 2005; Popescu et al., 2009).

Our objective is to investigate the palynological organic matter (POM) of the Neogene sediments, drilled by the Sidi Salim-1 well, onshore Nile Delta, to infer palaeoenvironments and evaluate its potential as hydrocarbon source rocks. The interval presumably occupied by the MSC in the present investigated well (i.e., Qawasim Formation, Messinian) was regarded as almost barren of biotic remains (Ouda and Obaidalla, 1995). We use the presently recovered organic-walled microfossils (mainly pollen, spores, and dinoflagellate cysts) to reconstruct the oceanographic conditions of the southeast Mediterranean during that time. We provide a north-south correlation between the present Neogene onshore palaeoenvironments and those recently established from the offshore Nile Delta (Mahmoud et al., 2024). Upon which, we aim to discuss our findings in the light of the recently discovered seismic-based riverine sediments in the nearby Levant Basin (Madof et al., 2019).

2. Geological setting

The Nile Delta area (Fig. 1) occupies an area of approximately 22,000 km² along the northeastern margin of the African plate. Tectonics in the Nile Delta area induced facies variations because of development of several palaeo-highs and lows. It lies on the slightly deformed outer northern margin of this African Plate. Major structural features seem to control its sedimentary regime (e.g., Sarhan and Hemdan, 1994; Sestini, 1995; Kamel et al., 1998). The delta area can be differentiated into two deep offshore and an onshore geologic provinces. The onshore region, where the studied Sidi Salim-1 well is located, is divided by a flexure hinge line zone into two structural sedimentary sub-provinces: South Nile Delta block and North Nile Delta Basin (Abdel Aal et al., 1994, 2000). Continuous subsidence in the area resulted in the accumulation of thick Neogene sediments in the North Nile Delta Basin (Sestini, 1995). The deltaic sequence of the Nile Delta consists of two clastic units, separated by an unconformity related to the MSC events (Shalaby and Sarhan, 2023): the pre-Messinian (e.g., Hamouda and El-Gharabawy, 2019) and the post-Messinian (e.g., Sarhan et al., 2014) typical deltaic facies.

The Neogene–Quaternary palaeoenvironment in the Nile Delta was discussed on stratigraphical, sedimentological, palaeontological, and geophysical (seismic) bases (e.g., Rizzini et al., 1978; Leila et al., 2019; Shebl et al., 2019; Mahmoud et al., 2024). A composite Neogene–Quaternary stratigraphic column in the Nile Delta area (Fig. 2) is presented.

Different environmental settings were documented for the Neogene rock units in the Nile Delta area. The Sidi Salim Formation corresponds to a lower neritic and/or slope environment according to the palaeoecological characteristics of its fauna, with *Globorotalia menardii* and *Globorotalia* gr. *fohsi* (Rizzini et al., 1978) and palynofacies, including dinoflagellate cysts such as *Spiniferites* and *Lingulodinium* (Mahmoud et al., 2024). Leila et al. (2019) stated that the Qawasim Formation constitutes progradational deltaic system, from prodelta and distal delta front (distal deltaic facies) to proximal delta front and delta plain (proximal deltaic facies). The Qawasim Formation was deposited during the Messinian but was reworked during the Early Pliocene transgression (Sestini, 1989, as Messinian Abu Madi Formation). The Abu Madi Formation reflects a wide range of environments from continental, littoral to marine (inner to outer shelf) environments (e.g., Leila et al., 2019; Shebl et al., 2019; El-Kahawy et al., 2022; Mahmoud et al., 2024). Leila et al. (2019) described upward changing facies from continental, subaerial gravity flow and fluvial, to marginal marine (estuarine). Rizzini et al. (1978) stated that the Abu Madi Formation lies on a fairly pronounced erosion surface, which followed the deposition of Qawasim and Rosetta formations. On the onshore Nile Delta, the Abu Madi Formation reflects the progressive drowning of the incised valley, bounded at the base by an erosional unconformity, created by the late Messinian sea level drop, and at the top by a drowning unconformity, related to the Early Pliocene transgression (Metwalli et al., 2023). The Kafr El Sheikh Formation was believed to have accumulated in neritic to basinal settings (Rizzini et al., 1978; Zaghloul et al., 2001; El-Kahawy et al., 2022). Recently, Mahmoud et al. (2024) noted that the fully open marine environments were established in the top parts of this rock unit in the offshore area of the NDO B-1 well. For the Nile Delta area, a palaeogeographical map of the Middle Miocene (Langhian–Serravallian) (modified after Said, 1990), and a Late Miocene (Tortonian) map showing palaeoshorelines and inland areas, 11.6–7.25 Ma (modified after Ouda and Obaidalla, 1995), are presented (Fig. 3a, b).

The MSC period in the Mediterranean Realm has been regarded as being progressively isolated from the Atlantic Ocean, leading to widespread precipitation of gypsum (5.96–5.6 Ma), massive salt deposition (5.6–5.5 Ma) and a dramatic sea level fall followed by brackish water environments of “Lago-Mare” (Lake Sea) facies (e.g., Ruggieri, 1967; Hsü et al., 1973; Cita, 1982; Krijgsman et al., 1999, 2010; Hilgen et al., 2007; Krijgsman and Meijer, 2008; Roveri et al., 2008, 2014). An upper bathyal

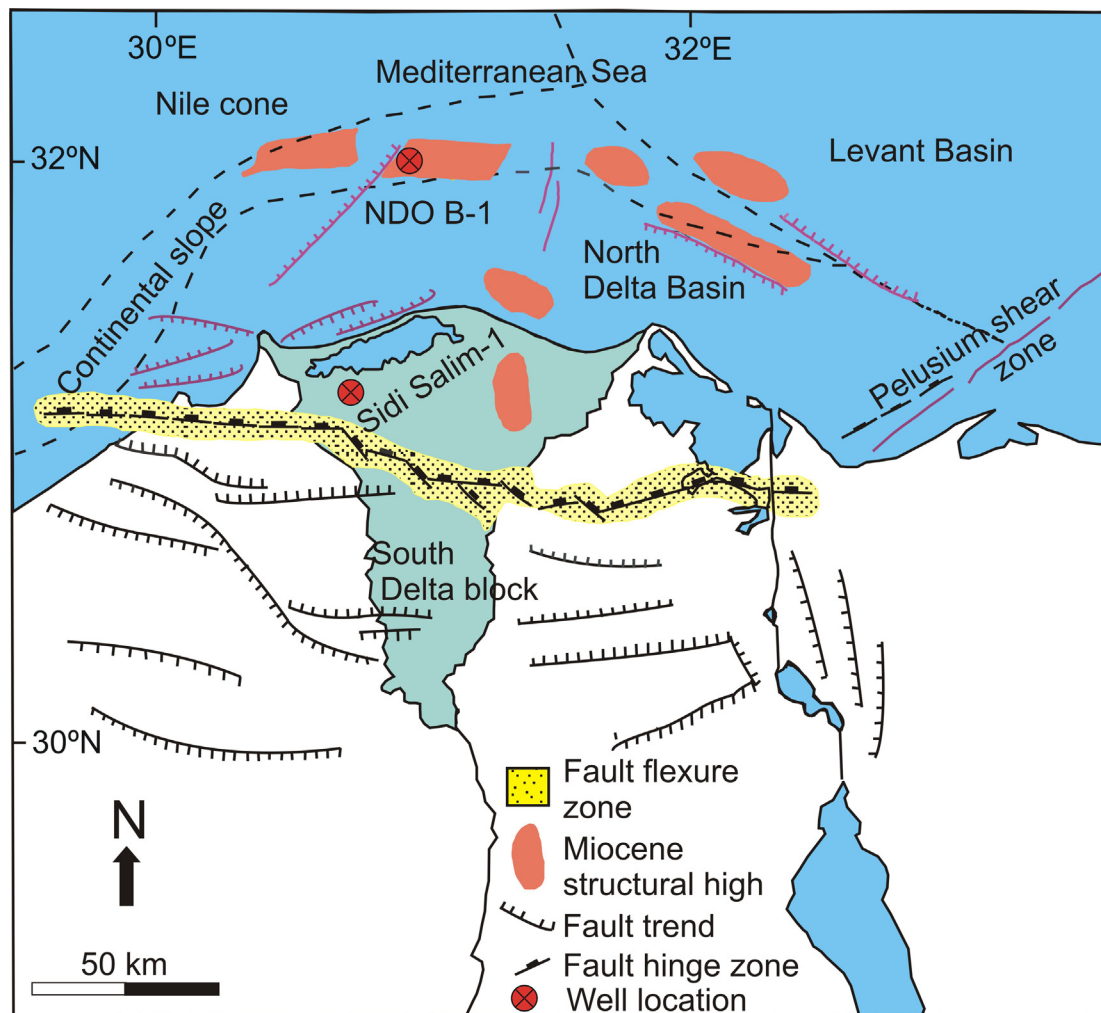


Fig. 1. Geographical map of the Nile Delta illustrating the location of the Sidi Salim-1 well, showing main structural and geomorphological features (modified after Barber, 1981; Sestini, 1989; redrawn from Makled et al., 2017).

environment existed before being driven to extinction during the Messinian salinity crisis (Hoffmann et al., 2020). A catastrophic re-flooding from the Atlantic at the beginning of the Pliocene (5.33 Ma) abruptly ended the MSC by retrieving open marine conditions in the Mediterranean through the Strait of Gibraltar, i.e., the Zanclean flood (e.g., Hsü et al., 1973; Garcia-Castellanos et al., 2020).

3. Lithostratigraphy

Rizzini et al. (1978) stated that the Nile Delta section is relatively uniform throughout the whole delta and consists of three sedimentary cycles: a Miocene cycle (Sidi Salem, Qawasim, and Rosetta formations) whose base is unknown; a Pliocene–Quaternary cycle (Abu Madi, Kafr El-Sheikh, El Wastani, and Mit Ghamr formations) and a Holocene cycle. There is no vertical sharp facies change between these deposits, which consist essentially of siliciclastic sediments. Regional correlation of these units, based upon lithology and geophysical logs, is not easy due to lack of sharp vertical facies changes, since they are made up

mainly of siliciclastic sediments (e.g., Farouk et al., 2014). The Neogene succession in the Sidi Salim-1 well (Fig. 4) is subdivided according to stratigraphic information presented in IEOC (1968), N.C.G.S. (1976), Rizzini et al. (1978), E.G.P.C. (1994) and Ouda and Obaidalla (1995). Independent planktonic foraminifera dating in the well is available (Ouda and Obaidalla, 1995). However, the Neogene rock units drilled by the investigated well is described as follows.

3.1. Sidi Salim Formation

Age: Middle to Late Miocene (Langhian–Tortonian) (Rizzini et al., 1978; Abdel-Kireem et al., 1984; Abdou et al., 1984; Ismail et al., 2010; Mandur and Makled, 2016; Makled et al., 2017).

This rock unit consists of clays with few intervals of dolomitic marls, sandstone and siltstone interbeds. Its thickness measures about 446 m in its type section of the Sidi Salim-1 well (Rizzini et al., 1978). Towards the southern delta it probably lies on the Moghra Formation or

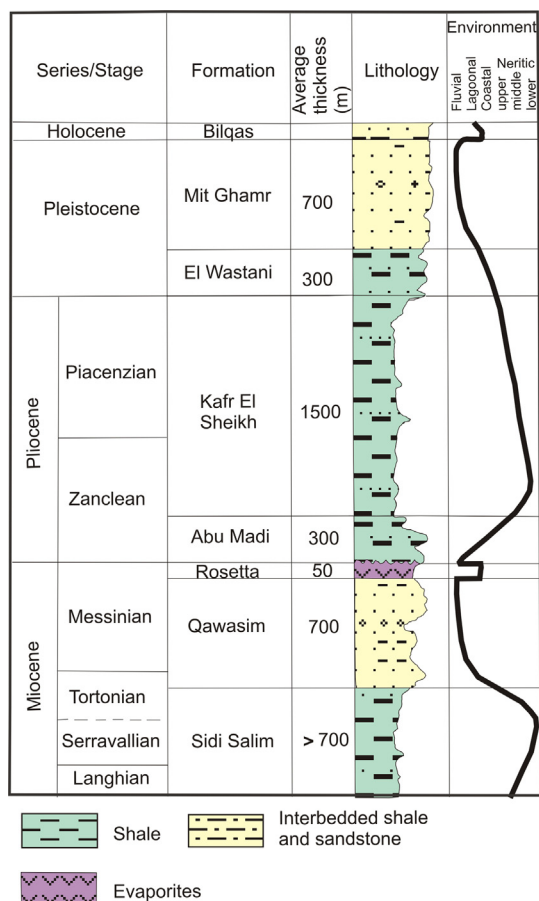


Fig. 2. Composite Neogene–Quaternary stratigraphic column in the Nile Delta, indicating average thicknesses and environmental trends of the examined formations (after Rizzini et al., 1978).

older rock units. In the offshore area of the delta, this rock unit is overlain by the Messinian Qawasim clastics and Rosetta anhydrites. In the present Sidi Salim-1 well, Ouda and Obaidalla (1995) recorded *Globorotalia mayeri*, *G. peripheroacuta*, *G. peripheroronda*, *Orbulina suturalis* and *Praeorbulina glomeroza*, equivalent to planktonic zones N8–N14, Middle Miocene (Langhian–Serravallian) of Blow (1969).

3.2 Qawasim Formation

Age: Late Miocene (Messinian) (Rizzini et al., 1978; Barber, 1981; Makled et al., 2017).

The formation consists of sand pebbles, sandstones and conglomerates (Rizzini et al., 1978), with a lenticular shape and slump structures. The Qawasim Formation type section is in the Qawasim-1 well (~933 m thick). At the base, the coarser sandy layers display erosional features. The conglomerates are generally massive and can show planar cross-beddings. Frequently there are layers of peat and coal fragments. The upper limit of this unit is difficult to define on the basis of subsurface data alone (Rizzini et al., 1978). A mixture of coastal-deltaic and fluvial deposits are widespread at the top of the formation, interbedded with

coastal (lagoons or swamps) deposits (e.g., Rizzini et al., 1978; El-Kahawy et al., 2022; Mahmoud et al., 2024). In the Sidi Salim-1 well, Ouda and Obaidalla (1995) recorded *Globigerinoides obliquus extremus* at the top of this rock unit.

3.3 Abu Madi Formation

Age: Early Pliocene (Zanclean) (Rizzini et al., 1978; Abdel-Kireem et al., 1984; Abdou et al., 1984; Ismail et al., 2010; Makled and Mandur, 2016; Makled et al., 2017).

The formation consists of thick layers (321 m in the Abu Madi well no. 1 type section) of sand and clay interbeds (Rizzini et al., 1978), with more frequent fauna-lacking conglomerates in the basal parts. Sands show large-scale cross-bedding and bioturbation is frequent in the clays. Foraminifera are frequent in the clay intervals and are typical of the Early Pliocene in the Mediterranean Sea (Cita, 1973). In the present Sidi Salim-1 well, Ouda and Obaidalla (1995) recorded *Sphaeroidinellopsis seminulina*, equivalent to the Early Pliocene (Zanclean) planktonic zone N18 of Blow (1969). Controversy exists regarding the designation and usage of rock units in the Neogene–Quaternary section of the Nile Delta area, particularly using the term Abu Madi Formation as equivalent to the Qawasim (Miocene) Formation.

3.4 Kafr El Sheikh Formation

Age: Pliocene (Zanclean–Piacenzian) (Rizzini et al., 1978; Abdel-Kireem et al., 1984; Abdou et al., 1984; Ismail et al., 2010; Makled and Mandur, 2016; Makled et al., 2017).

The age of this formation is easily defined with the occurrence of the *Globorotalia margaritae* and *G. punctulata* zones, Lower Pliocene, and the *G. aemiliana* and *G. crassaformis* zones, Middle Pliocene (Rizzini et al., 1978). In the present Sidi Salim-1 well, Ouda and Obaidalla (1995) recorded *G. margaritae*, equivalent to the planktonic zone N19 (Early Pliocene, Zanclean, of Blow, 1969). The type section is the Kafr El Sheikh well no. 1, about 1458 m thick. The fairly thick unit is widespread over the whole delta area and consists of clay and sand interbeds. The clays consist of kaolinite and montmorillonite, with minor illite (Rizzini et al., 1978). The Kafr El Sheikh Formation is conformably overlain by the El Wastani Formation.

4. Material and methods

We investigated the Neogene succession of the Sidi Salim-1 well (Figs. 1, 4), at the intersection of 31°19'10"N, 30°43'16"E, onshore Nile Delta, Egypt, drilled by IEOC (1968). Forty-one ditch samples were processed with HCl (35%) and HF (40%), according to the standard palynological processing techniques (e.g.,

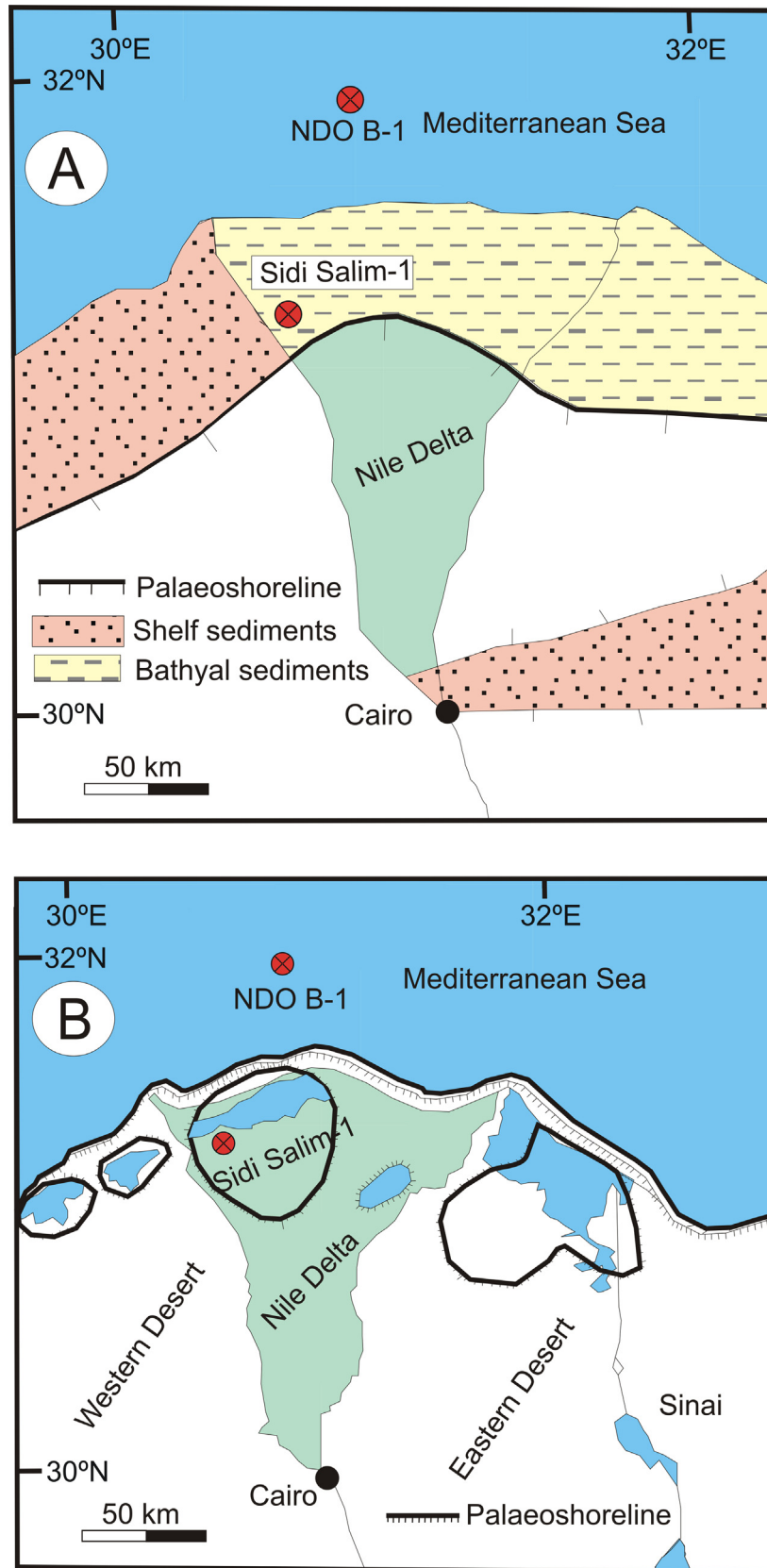


Fig. 3. (A) Palaeogeographical map of the Middle Miocene (Langhian–Serravallian) in the Nile Delta (modified after Said, 1990). (B) Palaeogeographical map of the Late Miocene (Tortonian) showing palaeoshorelines and inland areas, 11.6–7.25 Ma (modified after Ouda and Obaidalla, 1995).

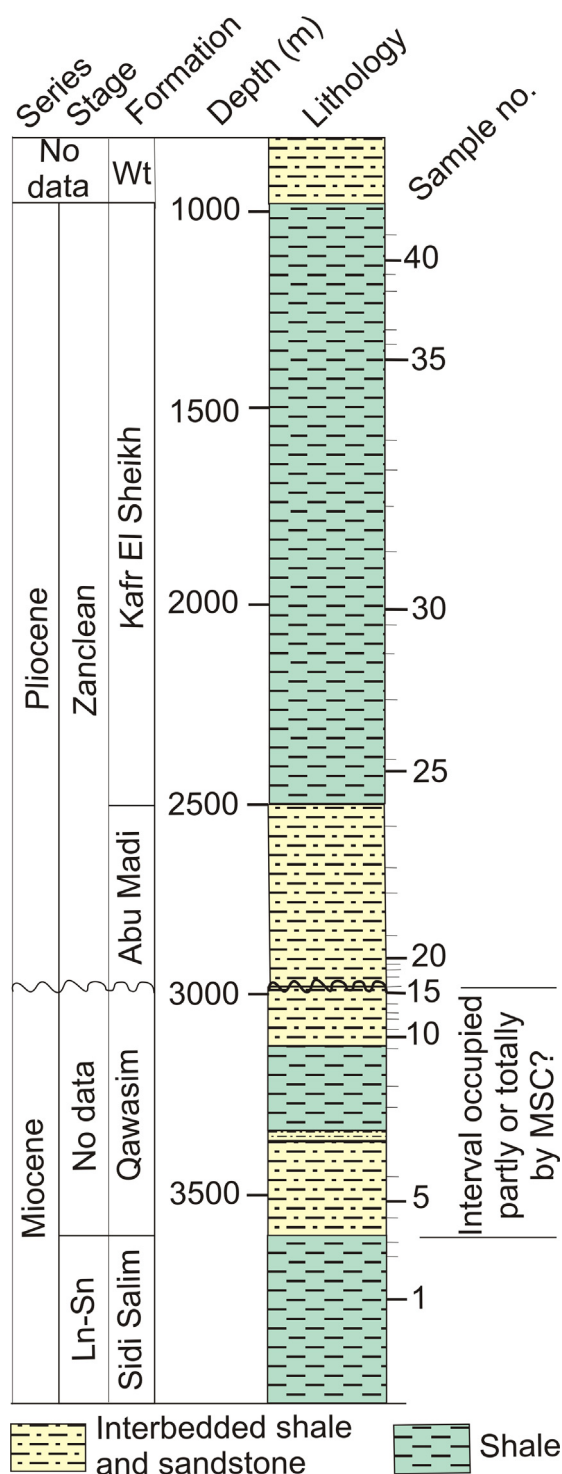


Fig. 4. Chrono- and lithostratigraphy of the Neogene succession in the investigated Sidi Salim-1 well, showing the stratigraphic location of studied samples. Rock units are subdivided according to information mainly presented in IEOC (1968), Rizzini et al. (1978) and Ouda and Obaidalla (1995). Relative ages in the Sidi Salim-1 well were taken from Ouda and Obaidalla (1995). Wt = El Wastani, Ln-Sn = Langhian–Serravallian.

Traverse, 2007), to remove carbonates and silicates, respectively. The digested residues were sieved through a 10 μ m mesh. This small size keeps the total digested POM from

being infiltrated throughout using the small-sized sieves. Oxidizing agents and/or ultrasonic vibration were avoided, to keep the total palynofacies unchanged. Then, part of the digested residue was gently treated with ultrasonic vibration for a few seconds to eliminate amorphous organic matter (AOM), which masks the recovery and concentration of palynomorphs (i.e., concentrated residue). For the light microscopic study, a set of permanent slides were prepared using glycerin jelly as a mounting medium. Slides were examined using a Leica DM LB2 light microscope equipped with a Leica DFC 280 digital camera at the Geology Department, Assiut University (Egypt). Representative examples of dinoflagellate cysts, pollen grains, spores and other palynological matter are illustrated in Figs. 5–7.

The processing techniques were performed to account for the relative abundances of the palynofacies categories (500 particles per sample) and palynomorphs (at least 200 palynomorphs per sample). The marine/continental (M/C) ratio was calculated as the number of marine palynomorphs (dinoflagellate cysts + microforaminiferal linings) divided by the sum of total palynomorphs $\times 100$. The palynological marine index (PMI) (Helenes et al., 1998) was calculated from the total recovered palynomorph content, using the formula $PMI = (R_m/R_t + 1) \times 100$, where R_m refers to the species richness of marine palynomorphs (dinoflagellate cysts and microforaminiferal linings) and R_t refers to the richness of terrestrial palynomorphs (pollen, spores and freshwater algae). *Pediastrum*/marine ratio was calculated as the number of the alga *Pediastrum* specimens divided by the sum of *Pediastrum* + dinoflagellate cysts + microforaminiferal linings (modified after Adeonipekun et al., 2023, since the alga *Botryococcus* is missing here). The above-mentioned counts of palynomorphs and palynofacies were used to create a set of graphic presentations to express the general framework of the palynological content. These counts were also applied to create ternary plots, to depict the palaeoenvironmental significance of palynomorphs (Federova, 1977; Düringer and Doubinger, 1985) and palynofacies (Tyson, 1993, 1995) and to recognize hydrocarbon potential (Dow, 1982). In addition, Origin-Lab software was used to create an R-mode hierarchical clustering of the palynofacies categories in order to provide insights supporting the visual characteristics of these components (Fig. 8).

5. Composition of palynofacies and palynomorphs

5.1. Palynofacies

The palynofacies of the Sidi Salim-1 well section fluctuates between phytoclast-dominated and AOM-rich categories (Fig. 8, 9A), Batten (1996) and Tyson (1993, 1995) were followed for terminology and description. Palynomorphs were extremely rare (maximum 1.5%, sample no. 40, Kafr El Sheikh Formation). Phytoclasts were the essential components of the palynofacies (more than 50% of the total kerogen), with an acme in samples no. 8

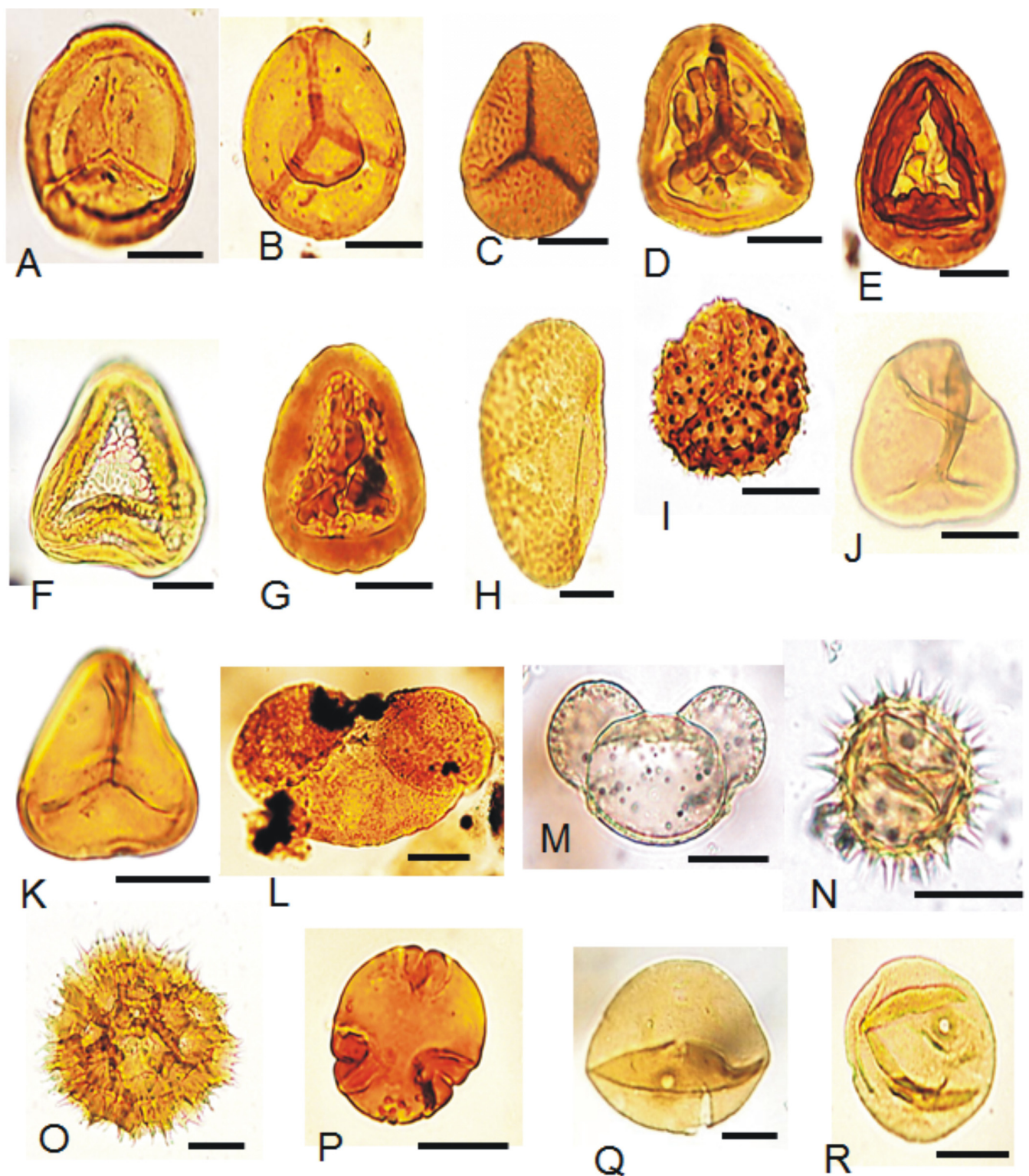
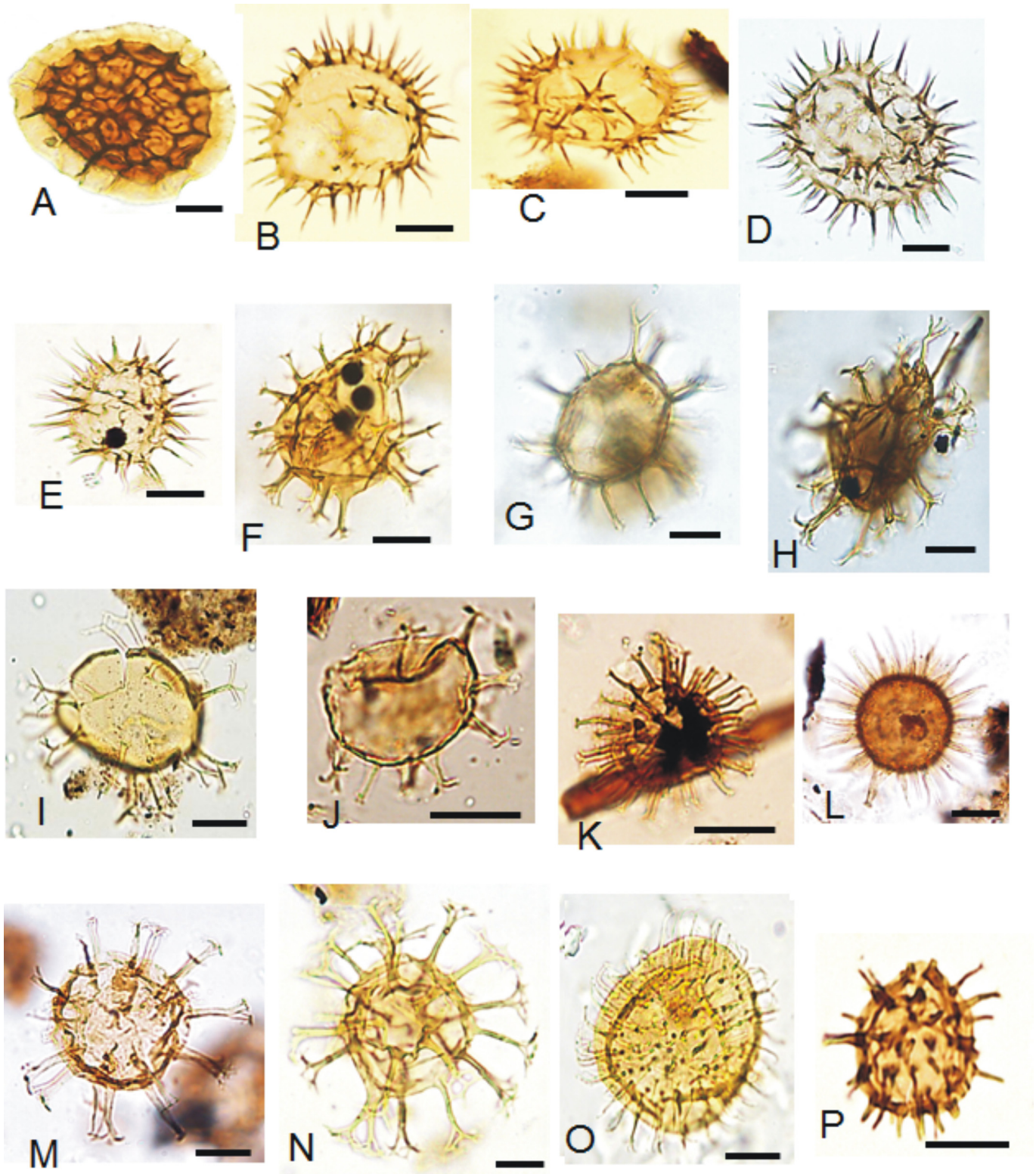


Fig. 5. Neogene spores and pollen, Sidi Salim-1 well, all photomicrographs, scale bar = 20 μ m. (A) *Polycingulatisporites* spp., depth: 2256 m, slide: c, sample no. 27, indices: 29.5/96.6. (B) *Annulispora salsa* Braman, depth: 2042 m, slide: c, sample no. 29, indices: 32.3/107.8. (C) Microreticulate spore, depth: 3567 m, slide: d, sample no. 4, indices: 39.5/95.1. (D–G) *Polypodiaceoisporites* spp.; (D) depth: 3567 m, slide: d, sample no. 4, indices: 49/114; (E) depth: 3033 m, slide: e, sample no. 13, indices: 31.9/104; (F) depth: 3064 m, slide: c, sample no. 11, indices: 32.2/110.2; (G) depth: 3567 m, slide: e, sample no. 4, indices: 44.7/96. (H) *Polypodiisporites speciosus* Sah *sensu* Mander et al., 2023, depth: 2987 m, slide: c, sample no. 17, indices: 29.8/102.9. (I) *Echinatisporis* sp., depth: 2134 m, slide: b, sample no. 28, indices: 38.8/95.2. (J) *Deltoidospora* sp. 2 Mander et al., 2023, depth: 2987 m, slide: a, sample no. 17, indices: 41.7/110.9. (K) *Deltoidospora* sp. 1 Mander et al., 2023, depth: 3567 m, slide: d, sample no. 4, indices: 41.3/108.8. (L, M) Bisaccate pollen; (L) depth: 2728 m, slide: b, sample no. 22, indices: 44.7/103.5; (M) depth: 3506 m, slide: c, sample no. 6, indices: 33.4/109.9. (N, O) Compositae (Asteraceae) pollen; (N) depth: 2134 m, slide: a, sample no. 28, indices: 37.3/106; (O) depth: 3048 m, slide: f, sample no. 12, indices: 33.2/102.8. (P) Tricolporate pollen?, depth: 2256 m, slide: a, sample no. 27, indices: 36.4/107.5. (Q, R) Poaceae (Gramineae) pollen; (Q) depth: 3064 m, slide: c, sample no. 11, indices: 42.2/107.3; (R) depth: 3567 m, slide: c, sample no. 4, indices: 43/97.2.



(60.7%, Qawasim Formation), no. 20 (79.1%, Abu Madi Formation) and no. 35 (63.1%, Kafr El Sheikh Formation). Phytoclasts, however, decline in a few horizons (e.g., 21.5%, sample no. 34, Kafr El Sheikh Formation). AOM is found in significant amounts (up to 78.1% of total palynofacies, sample no. 34). AOM lowest percentages occur in sample no. 20 (19.7%, Abu Madi Formation). Pyrite crystals were found imprinted over numerous palynomorph in most of the studied samples. These characteristics reflect a monotonous palynofacies with no clear vertical change that can allow differentiation. In the R-mode cluster analysis (Fig. 10), the palynofacies categories were classified into two clusters (A, B). Cluster A includes the essential palynofacies categories (phytoclasts and AOM), which constitute together the most abundant categories in most of the well interval. Cluster B, on the other hand, contains the rare palynofacies elements (marine palynomorphs and freshwater algae). Cluster A contains categories with related palynofacies derivation.

5.2. Palynomorphs

The palynomorph content of the well is masked by a large terrestrial palynofacies influx, related to the Nile River. However, counting the concentrated residue reflects dominance of terrestrial palynomorphs, such as spores, pollen, and freshwater algae, whereas marine elements are mostly minor (Fig. 8; Appendices 1, 2), as is evident from the low M/C ratio values. Freshwater algae were significant contributors to the Sidi Salim-1 well palynomorphs. At several horizons they reach an acme of 81% of total palynomorphs (sample no. 19, Abu Madi Formation, depth 2957 m). Land-derived spores and pollen grains were the essential components (up to 69.9%, sample no. 29, Kafr El Sheikh Formation, depth 2042 m). Spores reach up to 41% (sample no. 13, Qawasim Formation, depth 3033 m). They were dominated by trilete ferns whereas other monolet ferns were subordinate. Pollen grains were abundant (up to 38%, sample no. 38, Kafr El Sheikh Formation, depth 1243 m). Poaceae dominate the pollen association and occur in the majority of samples with percentages up to 17.5% (sample no. 38, Kafr El Sheikh Formation, depth 1243 m); their abundance sometimes declines to 0.65% (sample no. 24, top Abu Madi Formation, depth 2545 m). Dinoflagellate cysts, along with subordinate microforaminiferal linings, were not as abun-

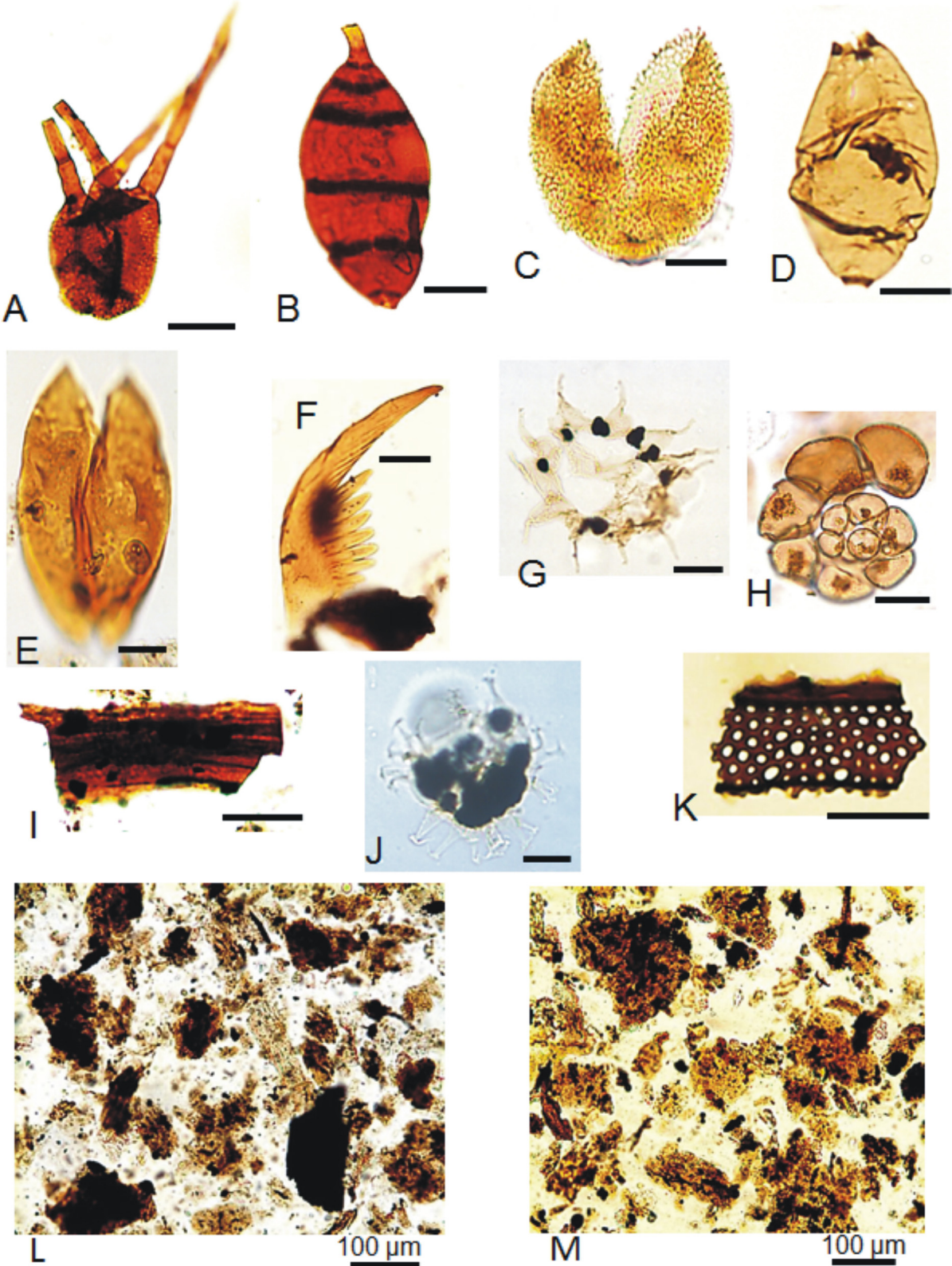
dant as terrestrial palynomorphs. They reach their maximum in three horizons in the Abu Madi Formation (48.7%, sample no. 22, depth 2728 m; 46.6%, sample no. 23, depth 2667 m; 55.7%, sample no. 24, depth 2545 m). Their abundance sometimes declines markedly or even disappears (sample no. 13, Qawasim Formation, depth 3033 m and sample no. 30, Kafr El Sheikh Formation, depth 2027 m). The PMI values generally range from 100 (sample no. 30, Kafr El Sheikh Formation, depth 2027 m) to 194.9 (sample no. 22, Abu Madi Formation, depth 2728 m). An increased value of the index (225.6) was documented at a depth of 2545 m (sample no. 24, near the top of Abu Madi Formation). The M/C ratio was generally low to moderate (0 to 48.7), with the exception of a single acme event (55.7) recorded in sample no. 24, corresponding to the highest PMI value. However, due to the masking/dilution of palynomorphs by the freshwater algae (mainly *Pediastrum*), the recovered palynomorphs were not presented semi-quantitatively. They were displayed qualitatively in two presence/absence distribution charts (Appendices 3, 4).

6. Palaeoenvironmental reconstruction

6.1. Inferences from environmental models of the POM

Basinal to shelf environments were inferred from the AOM–phytoclast–palynomorph (APP) ternary plot (Fig. 9A) of Tyson (1993, 1995). Nearly all samples fall in the fields VI and IX, which reflect oscillation from a proximal shelf to a distal basin and a suboxic-anoxic redox states. The higher percentages of AOM may refer to such basinal settings and may suggest a high preservation of autochthonous organic matter far from active sources of terrestrial matter (Tyson, 1995). The R-mode statistical analysis, cluster A (Fig. 10) shows that this AOM is linked with the abundant terrestrial components, namely brown and degraded wood phytoclasts, which may imply derivation partly from terrestrial sources. Some intervals have high phytoclasts and reflect periods of proximal setting, close to fluvio-deltaic sources of the land-derived organic matter. However, at a single horizon, near the top of the Abu Madi Formation, a marginal basinal environment was inferred, which is dysoxic-anoxic. The occurrence of pyrite (Fig. 7G, J), in the majority of the studied samples, confirms this anoxia, since pyrite can be absent in oxy-

Fig. 6. Neogene dinoflagellate cysts, Sidi Salim-1 well, all photomicrographs, scale bar = 20 μ m. (A) Indeterminable palynomorph, depth: 2993 m, slide: b, sample no. 16, indices: 46.5/106.9. (B–E) *Selenopemphix quanta* Bradford; (B) depth: 2993 m, slide: b, sample no. 16, indices: 41.3/99.9; (C) depth: 2993 m, slide: b, sample no. 16, indices: 44.6/103.8; (D) depth: 3018 m, slide: b, sample no. 14, indices: 26.3/110.4; (E) depth: 2987 m, slide: c, sample no. 17, indices: 30.9/103.9. (F–J) *Spiniferites* spp.; (F) depth: 2993 m, slide: a, sample no. 16, indices: 31.3/99.9; (G) depth: 3567 m, slide: a, sample no. 4, indices: 36.6/112.2; (H) depth: 2942 m, slide: b, sample no. 20, indices: 35.4/109.8; (I) depth: 1243 m, slide: a, sample no. 38, indices: 44.2/108.2; (J) depth: 1890 m, slide: b, sample no. 31, indices: 42.6/104.2. (K) cf. *Polysphaeridium* sp., depth: 2667 m, slide: b, sample no. 23, indices: 36/103.6. (L) *Lingulodinium machaerophorum* (Deflandre and Cookson) Wall, depth: 3292 m, slide: c, sample no. 7, indices: 38.5/101.3. (M, N) aff. *Melitasphaeridium* spp.; (M) depth: 3506 m, slide: a, sample no. 6, indices: 38.3/103.6; (N) depth: 2957 m, slide: o, sample no. 19, indices: 39.6/95.9. (O) *Operculodinium* sp., depth: 2987 m, slide: b, sample no. 17, indices: 22.8/96.1. (P) Indeterminable dinoflagellate cyst (cf. *Echinidinium* sp.), depth: 2942 m, slide: c, sample no. 20, indices: 32.6/109.



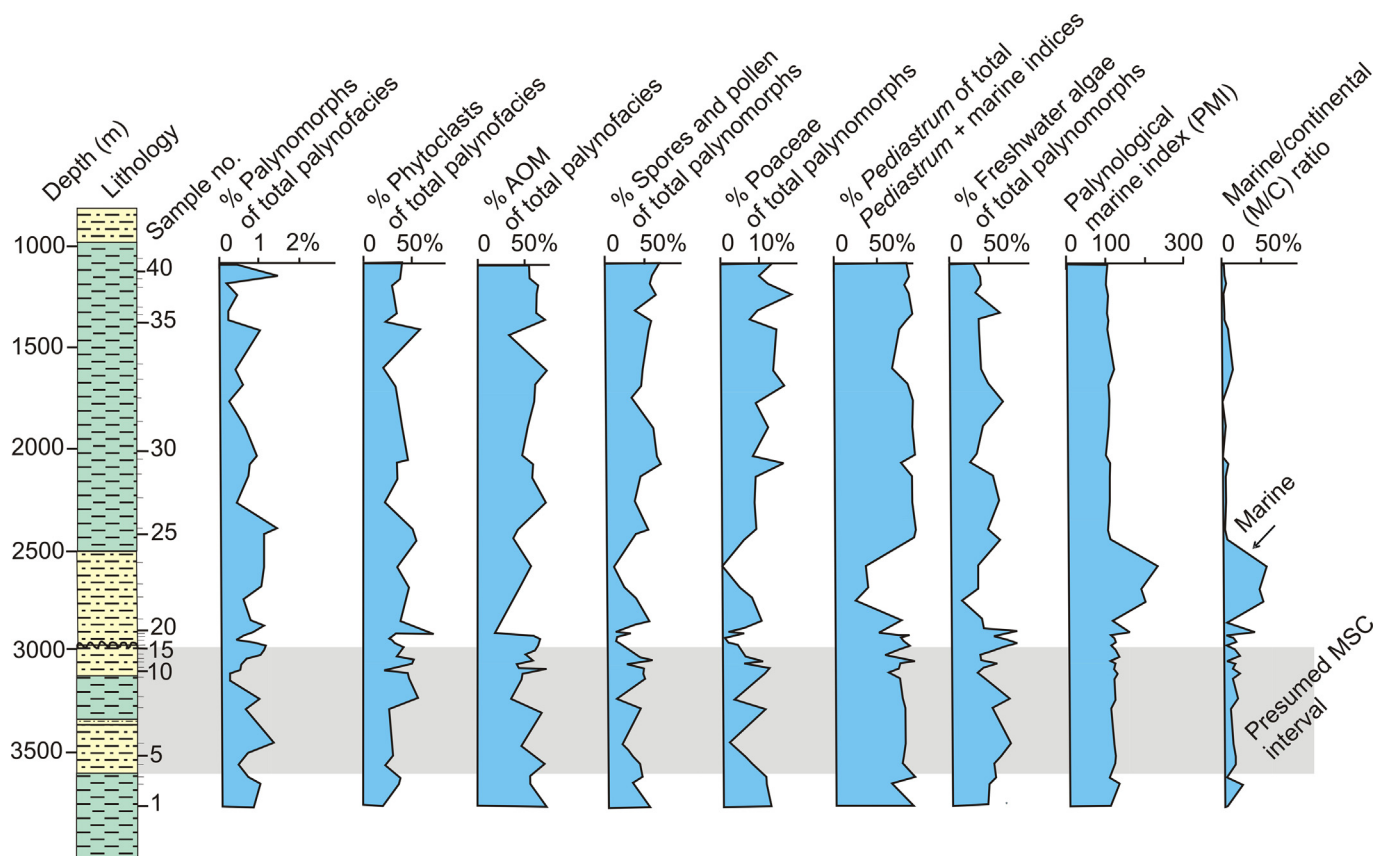


Fig. 8. Illustration of relative percentage frequency of the main palynofacies categories (palynomorphs, phytoclasts and AOM), terrestrial spores and pollen, Poaceae pollen, *Pediastrum* and freshwater algae in the Sidi Salim-1 well. Palynological Marine Index (PMI) and marine/continental ratio (M/C) are also presented. For chrono- and lithostratigraphic information see Fig. 4.

generated conditions (e.g., Roncaglia and Kuijpers, 2006). Consistent with pyrite, *Selenopemphix quanta*, which is an oxygen-sensitive dinoflagellate cyst (Zonneveld et al., 1997, 2001, 2007), occurs in most of the samples (Appendix 5). The presence of appreciable quantities of opaques in some horizons implies that they might have oxidized before their final destination in shelf/basin sites.

More details can be established by plotting the data on the microplankton–spore–pollen (MSP) ternary plot (modified after Federova, 1977; Düringer and Döbinger, 1985). The graph (Fig. 9B) clearly reflects the occurrence of a wide range of environments, ranging from deltaic to offshore marine. The Sidi Salim Formation, at the base of the inves-

tigated well section, exhibits a nearshore to shallow marine environment. The overlying Qawasim Formation exhibits a general shallow marine nature. Few samples in this rock unit reveal deltaic setting (samples at depths 3094 m, 3033 m and 3018 m). The deeper offshore setting was observed in the Abu Madi Formation (samples at depths 2987 m, 2942 m, 2728 m, 2667 m and 2545 m), although the other samples of the formation show a shallower environment (samples at depths 2972 m, 2957 m and 2835 m). In the Kafr El Sheikh Formation, the shallow marine (samples at depths 1615 m, 1408 m and 1161 m) and nearshore (samples at depths 2423 m, 2256 m, 1768 m, 1685 m, 1353 m and 1243 m) environments were restored. In the

Fig. 7. Neogene miscellaneous palynomorphs and palynofacies, Sidi Salim-1 well, all photomicrographs, scale bar = 20 μ m (unless otherwise indicated). (A) *Frasnacritetrus conatus* Saxena and Sarkar *sensu* Soliman et al., 2023, depth: 3567 m, slide: c, sample no. 4, indices: 41.5/103.6. (B, D) Fungal spores; (B) depth: 2393 m, slide: a, sample no. 26, indices: 32.8/105.7; (D) depth: 3567 m, slide: a, sample no. 4, indices: 40/111.2. (C) *Schizosporis reticulatus* Cookson and Dettmann, depth: 2987 m, slide: b, sample no. 17, indices: 31.6/96.7. (E) *Ovoidites parvus* (Cookson and Dettmann) Nakoman, depth 3079 m, slide: b, sample no. 10, indices: 29.3/105.9. (F) Scolecodont, depth: 2042 m, slide: c, sample no. 29, indices: 30.5/103. (G) *Pediastrum* sp., showing imprinted pyrite crystals, depth: 2987 m, slide: a, sample no. 17, indices: 27.7/111.7. (H) Planispiral microforaminiferal test lining, depth: 2728 m, slide: a, sample no. 22, indices: 34.2/109.4. (I) Black and brown striped tracheidal phytoclasts, depth: 1615 m, slide: a, sample no. 34, indices: 39.2/100.2. (J) Spiniferate cyst, showing imprinted pyrite crystals, depth: 2987 m, slide: a, sample no. SS-17, indices: 34.1/110.1. (K) Tracheid, depth: 2993 m, slide: b, sample no. SS-16, indices: 43.1/103.9. (L) Phytoclast-dominated palynofacies, depth: 3064 m, slide: a, sample no. SS-11, indices: 36/104. (M) AOM-dominated palynofacies, depth: 3765 m, slide: b, sample no. SS-1, indices: 35/101.

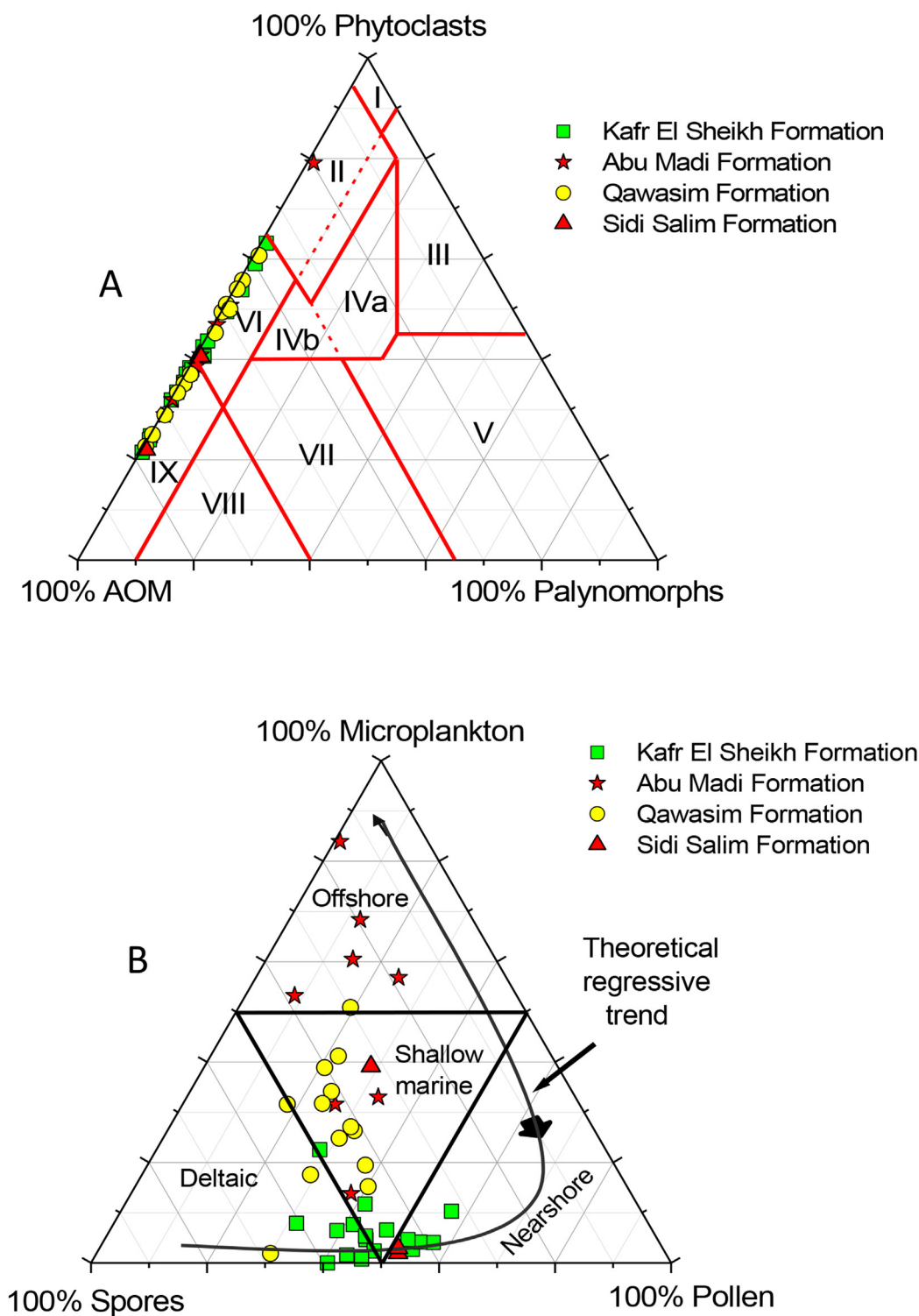


Fig. 9. (A) Ternary plot of samples in the Sidi Salim-1 well showing AOM–phytoclasts–palynomorphs (APP) diagram, based on relative numeric frequencies of main palynofacies components, with main palynofacies and environmental fields VI and IX, which refer to proximal shelf and distal basin settings, respectively (after Tyson, 1993, 1995). (B) Ternary plot of samples in the Sidi Salim-1 well showing microplankton–spores–pollen (MSP) diagram (after Federova, 1977; Düringer and Doubinger, 1985).

basal sediments of this rock unit, a deltaic environment terminated the offshore environments (samples at depths 2393 m, 2134 m, 2042 m, 2027 m, 1890 m, 1371 m, 1189 m and 1106 m) above the Abu Madi Formation.

6.2. Palaeoenvironmental significance of palynomorphs

The occurrence of *Spiniferites* spp. in the whole investigated succession (Appendix 5), along with *Selenopemphix*

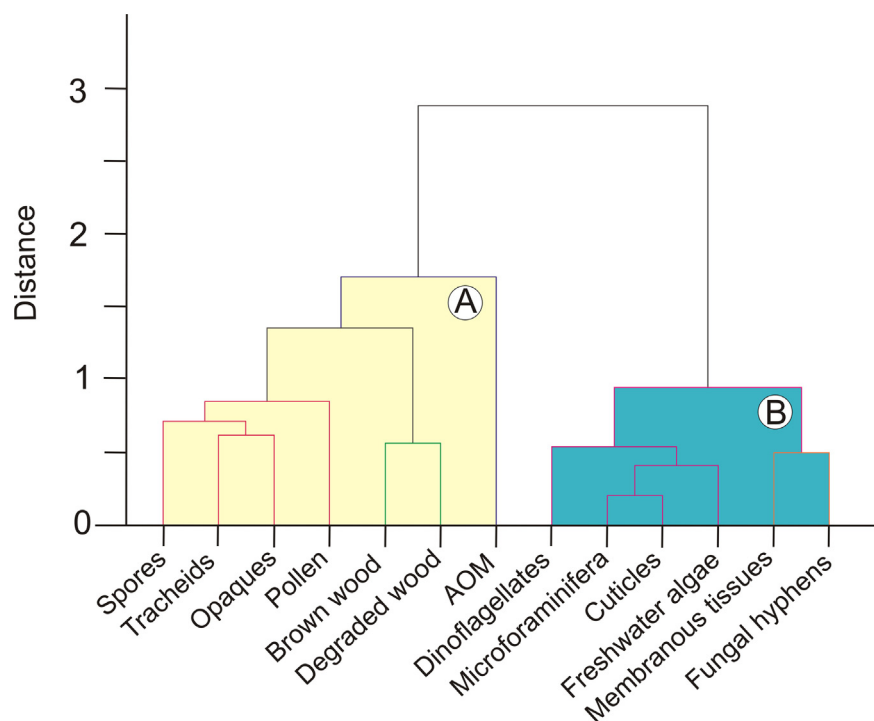


Fig. 10. Dendrogram of the R-mode cluster analysis of the palynofacies categories used in this study, Sidi Salim-1 well, based on data presented in Appendix 1. Cluster A contains the essential components of palynofacies, along with spores and pollen. Cluster B includes the dinoflagellate cysts and other secondary miscellaneous components.

spp., *Homotryblium* spp., *Operculodinium*, and *Hystri-chokolpoma* spp., is indicative of a marine environment (e.g., Dale, 1983; Mahmoud, 1993, 1998; Carvalho et al., 2016). *Spiniferites* spp. have high relative abundances in areas influenced by river discharge or in oligotrophic sites (Zonneveld et al., 2013). *Selenopemphix quanta*, *Lingulodinium machaerophorum* and *Spiniferites* spp. increase with the increasing nutrient/trace elements in coastal sites, near river plumes (Zonneveld et al., 2009). However, *S. quanta* occurs in coastal sites and near sub-tropical and equatorial front systems of polar to equatorial regions (Zonneveld et al., 2013). High abundances of *S. quanta* occur in eutrophic areas influenced by river discharge waters, but can be transported in large amounts from the shelf into deeper basins (Zonneveld and Brummer, 2000), where the upper waters may be of normal or reduced salinities. Highest relative abundances of this taxon can be found in regions characterized by anoxic to oxic bottom waters (Zonneveld et al., 2013). *Selenopemphix nephroides* (absent here) has not been observed in river plume areas (Zonneveld et al., 2013), although its low values may reflect neritic conditions with weak deltaic influence (Matthiessen and Brenner, 1996). The absence of *S. nephroides* in the present samples reflects the impact of a river plume, in contrast to that observed in the far northern offshore Nile Delta (Mahmoud et al., 2024, NDO B-1 well). This can also be explained in terms of the occurrence of Miocene structural highs (e.g., Sarhan and Hemdan, 1994; Sestini, 1995; Kamel et al., 1998) in the northern basins of the delta

(Fig. 1), where structural features control its sedimentation framework. Remarkably, *S. nephroides* was found in the Neogene sediments of the Nile Delta area but at its extreme eastern and western reaches (El Beialy, 1988, 1990a, 1992). *S. nephroides* occurrences in such peripheral positions are most probably due to a minimal river plume influence. *L. machaerophorum* is restricted to coastal regions and those close to terrestrial landscapes; its ordinary process lengths in the present samples are indicative of a normal marine salinity (Mertens et al., 2009; Zonneveld et al., 2009, 2013).

Poaceae (Gramineae) pollen is a Nilotic indicator, which is known to increase at the time of the Nile River flooding (Cheddadi and Rossignol-Strick, 1995; Kholeif, 2004). This pollen in the investigated samples possesses variable pollen sizes and is difficult to use alone as a proxy for reconstructing past vegetation and climate (Wei et al., 2023), although it is abundant in fossil records and often used as a palaeoclimatic indicator. Unfortunately, there are also problems associated with the morphological similarities across the Poaceae family, which prevent full use of their ecologic preferences. Usually, there are also difficulties in visually differentiating between different species of this pollen type (Katsi et al., 2024). A common interpretation is to link the increase in the Poaceae pollen abundance with increasing regional aridity. Poaceae distribution is influenced by various factors, such as the proportion, for example, of the size of local marshes (Bush, 2002). However, the relatively abundant Poaceae pollen in the majority our samples can be used as evidence of landscapes such as grassland,

open steppe, savanna or open desert lowlands (e.g., Germeraad et al., 1968; Hooghiemstra et al., 1986; Cheddadi and Rossignol-Strick, 1995; Davis, 1995; Cupper et al., 2000; Effiom et al., 2024) and, probably, a regional dry climates (e.g., Morley, 1995; Effiom et al., 2024). This explains the abundance of dinoflagellates in the Abu Madi Formation, probably due to an eutrophic state caused by the influence of a large terrigenous influx, rather than being associated with suboxic-anoxic states (Kang et al., 2025).

The low values of the M/C ratio (Fig. 8) reflect proximal/distal trends for the Neogene well section, since this ratio increases offshore (e.g., Pellaton and Gorin, 2005; Carvalho et al., 2013, 2016). Exceptionally, the highest values of this ratio in the Abu Madi Formation (48.7%, sample no. 22, depth 2728 m; 46.6%, sample no. 23, depth 2667 m; 55.7%, sample no. 24, depth 2545 m) refer to a deeper marine setting. The PMI values clearly reflect this, ranging between 100.3 (sample 26, depth 2393 m) and 126.5 (sample 2, depth 36.58 m). The highest values of the PMI were similarly observed in the same Abu Madi Formation (up to 194.9, sample no. 24, depth 2545 m).

7. The Miocene–Pliocene transition and the MSC

The boundary between Abu Madi (Lower Pliocene) and Qawasim (Upper Miocene) formations, is bounded by a pronounced erosional surface in the Nile Delta area (Rizzini et al., 1978). The Abu Madi Formation was described as bounded at the base and top by erosional and drowning unconformities, respectively, interpreted as reflecting the progressive drowning of an incised valley (Metwalli et al., 2023), related to a catastrophic sea-level fall (i.e., MSC) during the late Messinian. The higher PMI values (range from 118.7 to 225.5) and M/C ratios (range from 15.7 to 55.7) of the Abu Madi Formation, in the present investigated Sidi Salim-1 well, confirm this model. Correlation of the interval presumably occupied by the MSC in Sidi Salim-1 well (Qawasim Formation) is with that of the NDO B-1 well (Qawasim and Rosetta formations, Mahmoud et al., 2024), the latter is located about 97 km in a NNE direction, and showed that the thickness of Messinian rock units decreases northwards (Fig. 11). This correlation was based on the biostratigraphic results presented in Ouda and Obaidalla (1995) and Makled et al. (2017). The reason is that the NDO B-1 well lies on a Miocene structural high (Fig. 1), although it was drilled in the deeper northern basinal areas of the delta. This situation explains also why the above-mentioned drowning was not inferred in the NDO B-1 well.

The identification of the MSC event(s) and the provenance of marine palynomorphs are more problematic. However, missing of the lower evaporites and the resedimented lower gypsum (stages 1 and 2), in the Sidi Salim-1 well, may suggest “Lago Mare” substage 3.2 (Qawasim Formation). At the end of the Miocene, freshwater influx arrived from the brackish Eastern Paratethys and the

major peri-Mediterranean freshwater drainage systems from, for example, African rivers (e.g., Griffin, 2002). In the present work, fluvial discharge influence, which characterizes Substage 3.2 ‘Lago-Mare’, recently comprehensively reviewed by Andreetto et al. (2021), can be interpreted by the occurrence of a high percentage of *Pediastrum*, related to the Nile waters, not only in the Messinian but also across the whole Neogene interval of the well (e.g., Bertini, 2006). The marine setting of the Messinian interval, as evidenced by the occurrence of indigenous dinoflagellate cysts (e.g., *Spiniferites*, *Lingulodinium*, *Operculodinium*, *Selenopemphix*) seems to favour the deep non-desiccated basin hypothesis (e.g., Roveri et al., 2014; Krijgsman et al., 2018). However, Mahmoud et al. (2024) did not exclude the deep desiccated basin hypothesis (e.g., Hsü et al., 1973; Lofi et al., 2008; Madof et al., 2019) due to the occurrence of a widespread regional unconformity in the Nile Delta area, separating the two main (Miocene and Pliocene) clastic successions at the top of the Messinian (e.g., Metwalli et al., 2023; Shalaby and Sarhan, 2023). This possibility was suggested by Mahmoud et al. (2024) in the offshore Nile Delta area, NDO B-1 well, where there is an available planktonic dating, at the base of a non-distinctive zone, documented in this well by Makled and Mandur (2016) and Makled et al. (2017). This Mediterranean zone was dated by Lourens et al. (2004) at 5.96 Ma, implying that this interval in the NDO B-1 well witnessed the MSC events. But, due to the lack of a precise age dating for the Rosetta/Qawasim formations the relation of this interval, in these two wells, to a definite stage of the MSC is not possible. On the other hand, the relation of the Qawasim Formation in the present Sidi Salim-1 well to the MSC is highly enigmatic due to such age constraints, for example whether this interval is lower or upper Messinian. Consequently, the relation of the discovered vast Messinian terrestrial (riverine) deposits (Madof et al., 2019; Menashe River, in the nearby Levant Basin), to these Messinian Qawasim/Rosetta formations in the Nile Delta area (NDO B-1 and Sidi Salim-1 wells) seeks a plausible explanation. The absence of *Galeacysta etrusca* can suggest absence of Lago Mare interval sediments, in consistency with the widespread regional unconformity in the Nile Delta area. It is considered a marker for the uppermost Miocene (Magyar et al., 1999). Furthermore, the continuous presence of marine dinoflagellates, in the whole investigated succession of the Sidi Salim-1 well, cannot be applied to confirm the previously documented re-flooding of the Mediterranean Basin by Atlantic waters before the base of Pliocene (Zanclean) GSSP (e.g., Popescu et al., 2009), due to these age constraints.

8. Palynofacies and kerogen assessment

We used colours of the thin-walled spores (Fig. 12) and pollen for a visual assessment of the thermal maturity and the source-rock potential of the host sediments. Among the

different categories of POM, which have a potential in producing hydrocarbons, is the kerogen type II (oil-prone source material (e.g., Thompson and Dembicki, 1986; Tyson, 1995; Batten, 1996). The inferred suitable anoxic states are among the favorable conditions for the generation and preservation of organic matter (Wang et al., 2024). The thin-walled palynomorphs are usually applied to infer the spore coloration index (SCI), using the standard colour chart adapted after Pearson (1984) and numerical scales (e.g. Fisher et al., 1980; Collins, 1990). The colours of the present thin-walled trilete spores range from 5 to 8, which indicate thermally mature kerogen components. However, contradictory results were documented by Ibrahim (1996), from El Qara-2 well, northeast Nile Delta. He documented an increase in maturation of the POM in the Abu Madi Formation (metamorphosed), a mature interval corresponding to the lower Kafr El Sheikh

Formation and an immature interval in the upper Kafr El Sheikh Formation. Further investigation is recommended in the area to account for these different maturation states in the delta region. A possible explanation of the “metamorphosed” Abu Madi POM recorded by Ibrahim may be due to the impact of reworking in the area (Sestini, 1989; Mahmoud et al., 2024, fig. 9A) and the resultant mixing of the assemblages by older palynomorphs. However, on the ternary plot of Dow (1982), samples show potential of producing oil and wet gas + condensate (Fig. 13). In light of the above data, the succession is considered thermally mature and capable of producing oil and gas, consistent with organic geochemical results established by El Nady and Harb (2010) in the same Sidi Salim-1 well. Application of the same methodology used in Mahmoud et al. (2024), NDO B-1 well, offshore Nile Delta, has revealed the recognition of varying relative components of palyno-

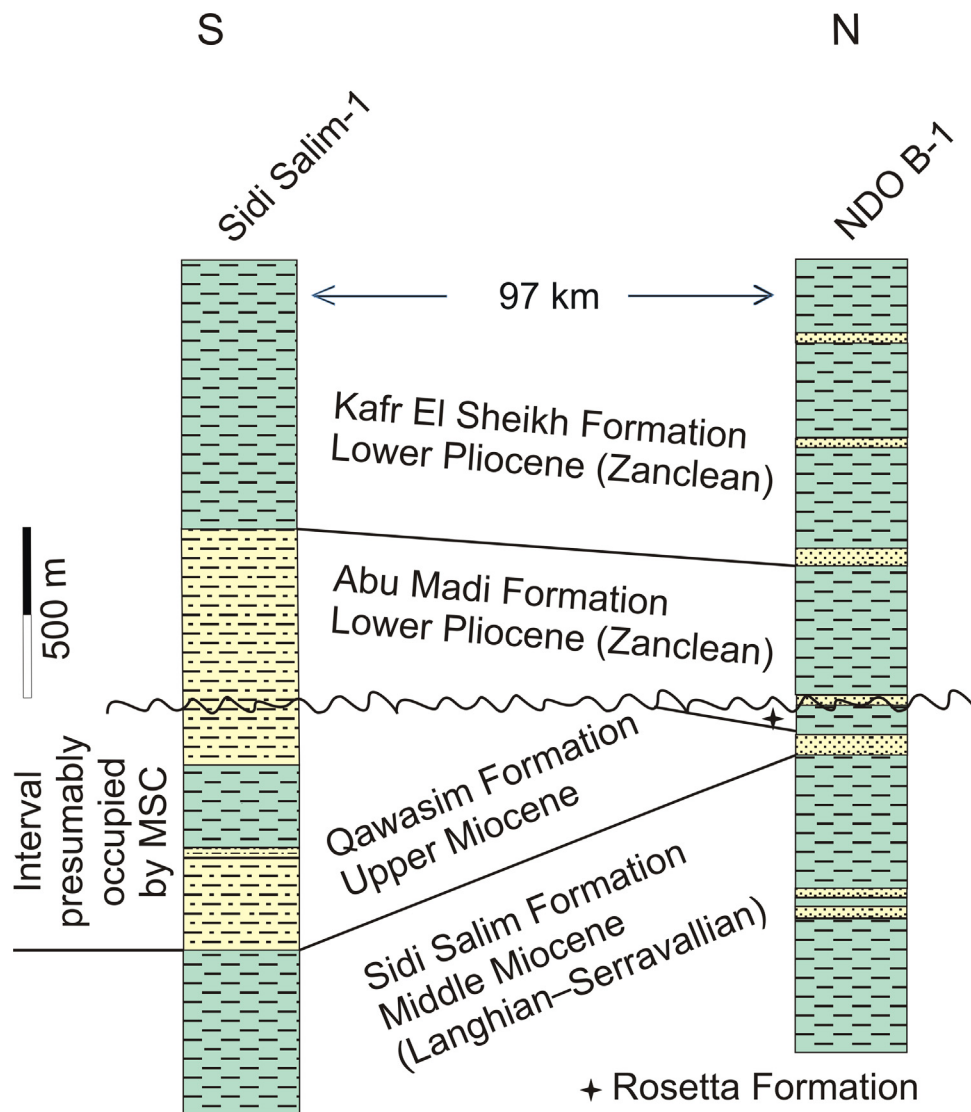


Fig. 11. Correlation of Neogene rock units penetrated by the Sidi Salim-1 well (onshore) and the NDO B-1 well (offshore, Mahmoud et al., 2024), in the northern Nile Delta area. Correlation based on biostratigraphic data presented in Ouda and Obaidalla (1995) and Makled et al. (2017). The unconformity surface at the Miocene–Pliocene boundary in the two wells was used as a datum.


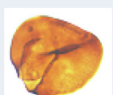
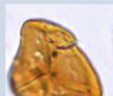

Formation	Thin-walled trilete spores	Organic thermal maturity & Equivalent SCI
Kafr El Sheikh		mature, 8
Abu Madi		mature, 7
Qawasim		mature, 6
Sidi Salim		mature, 5

Fig. 12. Illustration of organic thermal maturity and equivalent spore coloration index (SCI) of thin-walled trilete spores (after Fisher et al., 1980; Pearson, 1984; Collins, 1990).

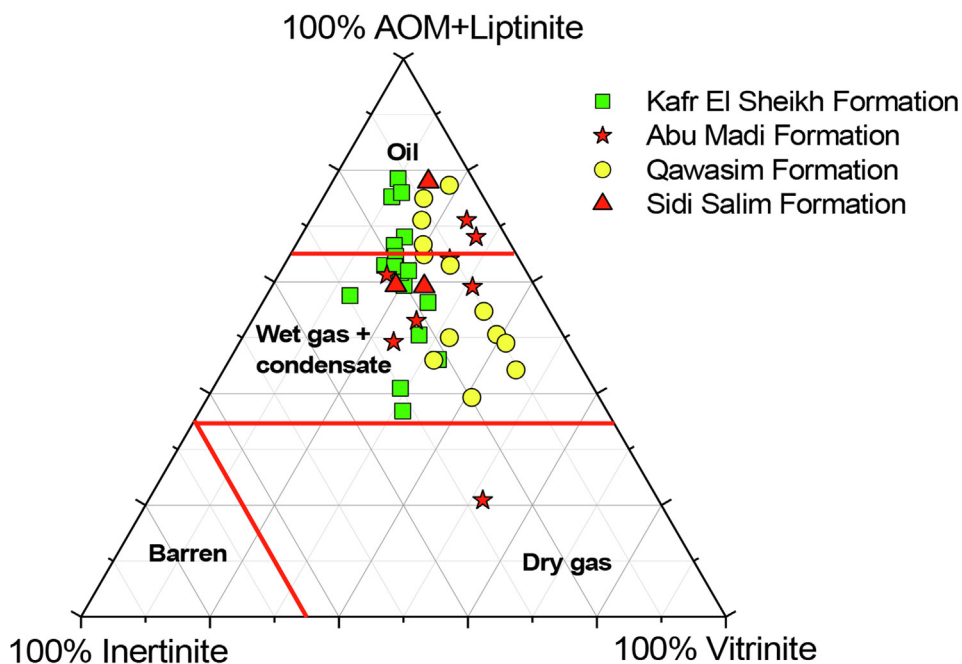


Fig. 13. AOM+Liptinite–Vitrinite–Inertinite (LVI) ternary kerogen diagram (after Dow, 1982), indicating fields of predicted hydrocarbon source potential, Sidi Salim-1 well.

facies, compared to the present investigated Neogene section of the Sidi Salim-1 well (Appendix 5). The deltaic influence and the offshore marine setting (Abu Madi Formation), in the present investigated well section, were more pronounced. This can be a result of the NDO B-1 well palaeogeographic position during Neogene. Environmental differences in this well are believed to have influenced the kerogen and the expected hydrocarbon types.

9. Conclusions

A near-shore environment was inferred in the Sidi Salim Formation and a deltaic to shallow marine environment was detected in the Qawasim and Kafr El Sheikh formations. The deeper (offshore) setting was established in the Abu Madi Formation, interpreted as reflecting the progressive drowning of an incised valley, related to a catastrophic

sea-level fall (i.e., MSC). Such basinal-shelf settings were confirmed by the occurrence of higher percentages of AOM. Dominance of phytoclasts reflects periods of more proximity to fluvio-deltaic sources of the organic matter. The occurrence of pyrite confirms the predominance of anoxia. The investigated organic matter is thermally mature, of the kerogen type II, which is capable of producing oil and gas.

Declaration of competing interest

The authors declare that they have no known competing financial interests or personal relationships that could have appeared to influence the work reported in this paper.

Acknowledgements

The authors thank the authorities of the Egyptian General Petroleum Corporation (E.G.P.C), for providing the samples and well logs for the present work. We thank D. Harper (Editor-in-Chief, Palaeoworld) for handling during the review process. Thanks are also due to A. Soliman (Tanta University, Egypt) and a second anonymous reviewer for their helpful comments that improved the manuscript. We thank A. Metwally (Geology Department, Assiut University) for conducting the statistical analysis.

Supplementary data

Supplementary data to this article can be found online at <https://doi.org/10.1016/j.palwor.2025.200966>.

References

- Abdel Aal, A., Price, R.J., Vaitl, J.D., Shallow, J.A., 1994. Tectonic evolution of the Nile Delta, its impact on sedimentation and hydrocarbon potential. EGPC 12th Exploration and Production Conference 1, 19–34.
- Abdel Aal, A., El Barkooky, A., Gerrits, M., Meyer, H., Schwander, M., Zaki, H., 2000. Tectonic evolution of the Eastern Mediterranean Basin and its significance for hydrocarbon prospectivity in the ultra deepwater of the Nile Delta. *The Leading Edge* 19 (10), 1086–1102.
- Abdel-Kireem, M.R., Abdou, H.F., Samir, A.M., 1984. Pliocene biostratigraphy and palaeoclimatology of the Buseili-IX well, Nile Delta, Egypt. *Neues Jahrbuch für Geologie und Paläontologie, Monatshefte* 1984 (10), 577–593.
- Abdou, H.F., Abdel-Kireem, M.R., Samir, A.M., 1984. Neogene planktonic foraminiferal biostratigraphy of Nile Delta. *Géologie Méditerranéenne* 11 (2), 193–205.
- Adeonipekun, P.A., Adeleye, M.A., Adebay, M.B., Sowunmi, M.A., 2023. The potentials of accessory palynomorphs as sequence stratigraphic and basin evaluation tools in the shallow offshore Niger Delta. *Review of Palaeobotany and Palynology* 318, 104985.
- Andreotto, F., Aloisi, G., Raad, F., Heida, H., Flecker, R., Agiadi, K., Lofi, J., Blondel, S., Bulian, F., Camerlenghi, A., Caruso, A., Ebner, R., Garcia-Castellanos, D., Gaullier, V., Guibourdenche, L., Gvirtzman, Z., Hoyle, T.M., Meijer, P.T., Moneron, J., Sierro, F.J., Travan, G., Tzevahirtzian, A., Vasiliev, I., Krijgsman, W., 2021. Freshening of the Mediterranean Salt Giant: controversies and certainties around the terminal (Upper Gypsum and Lago-Mare) phases of the Messinian Salinity Crisis. *Earth-Science Reviews* 216, 103577.
- Barber, P.M., 1981. Messinian subaerial erosion of the proto-Nile Delta. *Marine Geology* 44, 253–272.
- Batten, D.J., 1996. Palynofacies and palaeoenvironmental interpretation. In: Jansonius, J., McGregor, D.C. (Eds.), *Palynology: Principles and Applications*. American Association of Stratigraphic Palynologists Foundation, Dallas, pp. 1011–1064.
- Bertini, A., 2006. The Northern Apennines palynological record as a contribute for the reconstruction of the Messinian palaeoenvironments. *Sedimentary Geology* 188–189, 235–258.
- Blow, W. H., 1969. Late Miocene to Recent planktonic foraminifera biostratigraphy. In: Bronnimann, P., Renz, H.H. (Eds.), *Proceedings of the 1st International Conference on Planktonic Microfossils*. Vol. 1. E. J. Brill, Geneva, pp. 199–422.
- Bush, M.B., 2002. On the interpretation of fossil Poaceae pollen in the lowland humid neotropics. *Palaeogeography, Palaeoclimatology, Palaeoecology* 177, 5–17.
- Carvalho, M.A., Ramos, R.R.C., Crud, M.B., Witovisk, L., Kellner, A. W.A., Silva, H.P., Grillo, O.N., Riff, D., Romano, P.S., 2013. Palynofacies as indicators of paleoenvironmental changes in a Cretaceous succession from the Larsen Basin, James Ross Island, Antarctica. *Sedimentary Geology* 295, 53–66.
- Carvalho, M.A., Bengtson, P., Lana, C.C., 2016. Late Aptian (Cretaceous) paleoceanography of the South Atlantic Ocean inferred from dinocyst communities of the Sergipe Basin, Brazil. *Paleoceanography* 31, 2–26.
- Cheddadi, R., Rossignol-Strick, M., 1995. Eastern Mediterranean Quaternary paleoclimates from pollen and isotope records of marine cores in the Nile cone area. *Paleoceanography* 10, 291–300.
- Cita, M.B., 1973. Pliocene biostratigraphy and chronostratigraphy. *Initial Reports of the Deep Sea Drilling Project* 13, 1343–1379.
- Cita, M.B., 1982. The Messinian salinity crisis in the Mediterranean: a review. *Alpine-Mediterranean Geodynamics* 7, 113–139.
- Clauzon, G., Suc, J.-P., Popescu, S.-M., Marunteanu, M., Rubino, J.-L., Marinescu, F., Melinte, M.C., 2005. Influence of the Mediterranean sea-level changes over the Dacic Basin (Eastern Paratethys) in the Late Neogene: The Mediterranean Lago Mare facies deciphered. *Basin Research* 17, 437–462.
- Collins, A., 1990. The 1-10 spore colour index (SCI) scale: a universally applicable colour maturation scale, based on graded, picked palynomorphs. In: Fermont, W.J.J., Weegink, J.W. (Eds.) (Eds.). *Mededelingen Rijks Geologische Dienst* 45, 39–47.
- Copper, M.L., Drinnan, A.N., Thomas, I., 2000. Holocene palaeoenvironments of salt lakes in the Darling Anabranch region, South-Western New South Wales, Australia. *Journal of Biogeography* 27, 1079–1094.
- Dale, B., 1983. Dinoflagellate resting cysts: benthic plankton. In: Fryxell, G.A. (Ed.), *Survival Strategies of the Algae*. Cambridge University Press, Cambridge, pp. 69–136.
- Davis, O., 1990. Climate and vegetation patterns in surface samples from arid Western U.S.A.: Application to Holocene climatic reconstructions. *Palynology* 19 (1), 95–117.
- Dow, W.G., 1982. Kerogen maturity and type by reflected light microscopy applied to petroleum exploration. In: Staplin, F.L., Dow, W.G., Milner, C.W.O., Milner, C.W.D., O'Connor, D.I., Pocock, S.A.J., Van Gijssel, P., Welte, D.H., Yukler, M.A. (Eds.), *How to Assess Maturation and Paleotemperatures*. Society of Economic Paleontologists and Mineralogists Short Course 7, 133–157.
- Düringer, P., Doubinger, J., 1985. La palynologie: un outil de caractérisation des faciès marins et continentaux à la limite Muschelkalk supérieur-Lettenkohle. *Sciences Géologiques, Bulletins et Mémoires* 38, 19–34.
- Effiom, A.C., Neumann, F.H., Bamford, M.K., Scott, L., 2024. Mid-Late Holocene palynological development at Lake St Lucia, KwaZulu-Natal. *Review of Palaeobotany and Palynology* 322, 105046.
- E.G.P.C. (Egyptian General Petroleum Corporation), 1994. Western Desert, Oil and Gas Fields (A Comprehensive Overview). Egyptian General Petroleum Corporation, Cairo, 431 pp.

- El Atfy, H., 2021. Palynofacies as a paleoenvironment and hydrocarbon source potential assessment tool: An example from the Cretaceous of north Western Desert, Egypt. *Palaeobiodiversity and Palaeoenvironments* 101, 35–50.
- El Beialy, S.Y., 1988. Palynostratigraphy of late tertiary sediments in Kafr El Dawar well no. 1, Nile delta, Egypt. *Revue de Micropaléontologie* 30 (4), 249–260.
- El Beialy, S.Y., 1990a. Palynology, palaeoecology, and well dinocyst stratigraphy of the Oligocene through Pliocene succession in the Qantara-1 well, eastern Nile Delta, Egypt. *Journal of African Earth Sciences* 11 (3/4), 291–307.
- El Beialy, S.Y., 1990b. Tertiary dinoflagellates cysts from the Mit Ghamr-1 well, Nile Delta, Egypt. *Review of Palaeobotany and Palynology* 63, 259–267.
- El Beialy, S.Y., 1992. Miocene and Pliocene dinoflagellates cysts and other palynomorphs from the Damanhour South-1 well, western Nile Delta, Egypt. *Neues Jahrbuch für Geologie und Paläontologie, Monatshefte* 1992 (10), 577–594.
- El Beialy, S.Y., 1997. Dinoflagellates cysts, sporomorphs and other palynomorphs across the Miocene/Pliocene boundary, Kafr El Sheikh-1 well, Nile Delta, Egypt. *Neues Jahrbuch für Geologie und Paläontologie, Monatshefte* 1997 (7), 383–398.
- El Diasty, W.S., El Beialy, S.Y., El Attar, R.M., Khairy, A., Peters, K.E., Batten, D.J., 2019. Oil source correlation in the West Esh El Mellaha, southwestern margin of the Gulf of Suez rift, Egypt. *Journal of Petroleum Science and Engineering* 180, 844–860.
- El-Kahawy, R.M., Aboul Ela, N., El Barkooky, A.N., Kassab, W., 2022. Biostratigraphy and paleoenvironment implications of the Middle Miocene–Early Pliocene succession, El-Wastani gas field, onshore Nile Delta, Egypt. *Arabian Journal of Geosciences* 15, 341.
- El Nady, M.M., Harb, F.M., 2010. Source rocks evaluation of Sidi Salem-1 well in the onshore Nile Delta, Egypt. *Petroleum Science and Technology* 28 (14), 1492–1502.
- Farouk, S., Ziko, A., Eweda, A.S., Said, A.E., 2014. Subsurface Miocene sequence stratigraphic framework in the Nile Delta, Egypt. *Journal of African Earth Sciences* 9, 89–109.
- Federova, V.A., 1977. The significance of the combined use of microphytoplankton, spores, and pollen for differentiation of multi-facies sediments. In: Samoilovich, S.R., Timoshina, N.A. (Eds.), *Questions of Phytostратigraphy*. Trudy, Neftyanoi nauchnoissledovatel'skii geologorazvedochnyi Institut (VNIGRI) 398, 70–88 (in Russian).
- Fisher, M.J., Barnard, P.C., Cooper, B.S., 1980. Organic maturation and hydrocarbon generation in the Mesozoic sediments of the Sverdrup Basin, Arctic Canada. In: *Proceeding of the 4th International Palynological Conference*, Lucknow, 2, 581–588.
- Garcia-Castellanos, D., Micallef, A., Estrada, F., Camerlenghi, A., Ercilla, G., Perianez, R., Abril, J.M., 2020. The Zanclean megaflood of the Mediterranean – Searching for independent evidence. *Earth-Science Reviews* 201, 103061.
- Germeraad, J.H., Hopping, C.A., Muller, J., 1968. Palynology of Tertiary sediments from tropical areas. *Review of Palaeobotany and Palynology* 6, 189–348.
- Griffin, D.L., 2002. Aridity and humidity: two aspects of the late Miocene climate of North Africa and the Mediterranean. *Palaeogeography, Palaeoclimatology, Palaeoecology* 182 (1–2), 65–91.
- Hamouda, A., El-Gharabawy, S., 2019. Impacts of neotectonics and salt diapir on the Nile fan deposit, Eastern Mediterranean. *Environmental and Earth Sciences Research Journal* 6 (1), 8–18.
- Helenes, J., De-Guerra, C., Vazquez, J., 1998. Palynology and chronostratigraphy of the upper Cretaceous in the subsurface of the Barinas area, western Venezuela. *American Association of Petroleum Geologists Bulletin* 82, 1308–1328.
- Hilgen, F., Kuiper, K., Krijgsman, W., Snel, E., van der Laan, E., 2007. Astronomical tuning as the basis for high resolution chronostratigraphy: the intricate history of the Messinian Salinity Crisis. *Stratigraphy* 4 (2–3), 231–238.
- Hoffmann, R., Bitner, M.A., Pisera, A., Jäger, M., Auer, G., Giraldo-Gómez, V., Kočí, T., Buckeridge, J., Mueller, M., Stevens, K., Schneider, 2020. Late Miocene biota from the Abad Member of the Carboneras-Nijar Basin (Spain, Andalusia): A bathyal fossil assemblage pre-dating the Messinian salinity crisis. *Geobios* 59, 1–28.
- Hooghiemstra, H., Agwu, C.O.C., Beug, H.J., 1986. Pollen and spore distribution in Recent marine sediments: a record of NW-African seasonal wind patterns and vegetation belts. *Meteor. Forschungsgebeit Reihe* 40, 87–135.
- Hsü, K.J., Ryan, W.B.F., Cita, M., 1973. Late Miocene desiccation of the Mediterranean. *Nature* 242, 240–244.
- Ibrahim, M.I.A., 1996. Spore colour index and organic thermal maturation studies on the Pliocene sediments of the El Qara-2 Borehole, Nile Delta Area, Egypt. *Qatar University Science Journal* 16 (1), 167–172.
- IEOC (International Egyptian Oil Company), 1968. *Stratigraphical Reports of I.E.O.C. Wells Drilled in the Nile Delta*. Unpublished reports, I.E.O.C., Cairo.
- Ismail, A.A., Boukhary, M., Abdel Naby, A.I., 2010. Subsurface stratigraphy and micropaleontology of the Neogene rocks, Nile Delta, Egypt. *Geologica Croatica* 63 (1), 1–26.
- Kamel, H., Eita, T., Sarhan, M., 1998. Nile Delta hydrocarbon potentiality. *Proceedings of the 14th Egyptian General Petroleum Corporation Exploration and Production Conference*, Cairo, Egypt, pp. 485–503.
- Kang, J., Wang, X., Huang, Z., Huo, F., Li, Y., Zeng, D., Zhu, Y., Li, B., Xie, S., Chen, W., Huang, H., 2025. Influence of depositional environment on organic matter accumulation in lacustrine shales: the Jurassic Dongyemiao Member, Sichuan Basin, China. *International Journal of Earth Sciences* 114, 425–444.
- Katsi, F., Kent, M.S., Jones, M., Fraser, W.T., Jardine, P.E., Eastwood, W., Mariani, M., Osborne, C., Edwards, S., Lomax, B.H., 2024. FTIR spectra from grass pollen: A quest for species-level resolution of Poaceae and Cerealia-type pollen grains. *Review of Palaeobotany and Palynology* 321, 105039.
- Kholeif, S.E.A., 2004. Palynology and palaeovegetation reconstruction in late Quaternary sediments of the southern Suez Isthmus, Egypt. *Journal of African Earth Sciences* 22, 93–112.
- Krijgsman, W., Meijer, P.T., 2008. Depositional environments of the Mediterranean “Lower Evaporites” of the Messinian salinity crisis: constraints from quantitative analyses. *Marine Geology* 253 (3–4), 73–81.
- Krijgsman, W., Hilgen, F.J., Raffi, I., Sierro, F., Wilson, D.S., 1999. Chronology, Crisis and Progression of the Messinian Salinity Crisis. *Nature* 400, 652–655.
- Krijgsman, W., Stoica, M., Vasiliev, I., Popov, V.V., 2010. Rise and fall of the Paratethys Sea during the Messinian Salinity Crisis. *Earth and Planetary Science Letters* 290 (1–2), 183–191.
- Krijgsman, W., Capella, W., Simon, D., Hilgen, F.J., Kouwenhoven, T.J., Meijer, P.Th., Sierro, F.J., Tulbure, M.A., van den Berg, B.C.J., van der Schee, M., Flecker, R., 2018. The Gibraltar Corridor: Watergate of the Messinian Salinity Crisis. *Marine Geology* 403, 238–246.
- Leila, M., Moscariello, A., Šegvić, B., 2019. Depositional facies controls on the diagenesis and reservoir quality of the Messinian Qawasim and Abu Madi formations, onshore Nile Delta, Egypt. *Geological Journal* 54, 1797–1813.
- Lofi, J., Deverchère, J., Gaullier, V., Gillet, H., Gorini, C., Guennoc, P., Loncke, L., Maillard, A., Sage, F., Thion, I., Capron, A., Obone Zue Obame, E., 2008. The Messinian Salinity Crisis in the offshore domain: an overview of our knowledge through seismic profile interpretation and multi-site approach. In: Briand, F. (Ed.), *The Messinian Salinity Crisis from Mega-deposits to Microbiology – A consensus report*. CIESM, Monaco, pp. 83–90.
- Lourens, L.J., Hilgen, F.J., Shackleton, N.J., Laskar, J., Wilson, D., 2004. Appendix 2. Orbital tuning calibration and conversions for the Neogene Period. In: Gradstein, F.M., Ogg, J.G., Smith, A.G. (Eds.), *A Geologic Time Scale*. Cambridge University Press, Cambridge, pp. 469–484.
- Madof, A.S., Bertoni, C., Lofi, J., 2019. Discovery of vast fluvial deposits provides evidence for drawdown during the late Miocene Messinian salinity crisis. *Geology* 47, 171–174.

- Magyar, I., Geary, D.H., Sütö-Szentai, M., Lantos, M., Müller, P., 1999. Integrated bio-, magneto- and chronostratigraphic correlations of the Late Miocene Lake Pannon deposits. *Acta Geologica Hungarica* 42, 5–31.
- Mahmoud, M.S., 1993. Dinocyst stratigraphy of the Middle Miocene from Shagar-1 borehole, SW Gulf of Suez (Egypt). *Newsletters on Stratigraphy* 28 (1), 79–92.
- Mahmoud, M.S., 1998. Palynology of Middle Cretaceous–Tertiary sequence of Mersa Matruh-1 well, northern Western Desert, Egypt. *Neues Jahrbuch für Geologie und Paläontologie, Abhandlungen* 209 (1), 79–104.
- Mahmoud, M.S., Deaf, A.S., El Hussieny, M.-A.-T., 2024. Neogene–Quaternary paleoenvironments and kerogen assessment of the NDO B-1 well, offshore Nile Delta, Egypt, Eastern Mediterranean: palynological evidence. *Acta Geologica Polonica* 74 (3), e21.
- Makled, W.A., Mandur, M.M.M., 2016. Nannoplankton calendar: applications of nannoplankton biochronology in sequence stratigraphy and basin analysis in the subsurface offshore Nile Delta, Egypt. *Marine and Petroleum Geology* 72, 374–392.
- Makled, W.A., Mostafa, T., Maky, A., Baioumi, A., 2013. Palynological, palynofacies studies and hydrocarbon potentiality of middle Miocene–Pliocene rock units from the Nile Delta, Egypt. *International Journal of Academic Research* 5, 20–37.
- Makled, W.A., Mandur, M.M., Langer, M.R., 2017. Neogene sequence stratigraphic architecture of the Nile Delta, Egypt: a micropaleontological perspective. *Marine and Petroleum Geology* 85, 117–135.
- Mander, L., Jaramillo, C., Oboh-Ikuenobe, F., 2023. Descriptive systematics of Upper Palaeocene–Lower Eocene pollen and spores from the northern Niger Delta, south-eastern Nigeria. *Palynology* 47 (3), 2200525.
- Mandur, M.M.M., Makled, W.A., 2016. Implications of calcareous nannoplankton biostratigraphy and biochronology of the Middle–Late Miocene of the Nile Delta, Egypt. *Arabian Journal of Geosciences* 9, 203.
- Matthiessen, J., Brenner, W., 1996. Dinoflagellate cyst ecostratigraphy of Pliocene–Pleistocene sediments from the Yermak Plateau (Arctic Ocean, Hole 911A). *Proceedings of the Ocean Drilling Program, Science Results* 151, 243–253.
- Mertens, K., Ribeiro, S., Bouimatarhan, I., Caner, H., Combourieu-Nebout, N., Dale, B., De Vernal, A., Ellegaard, M., Filipova, M., Godhe, A., Goubert, E., Grøsfjeld, K., Holzwarth, U., Kotthoff, U., Leroy, S.A.G., Londeix, L., Marret, F., Matsuoka, K., Mudie, P.J., Naudts, L., Peña-Manjarrez, J.-L., Persson, A., Popescu, S.-M., Pospelova, V., Sangiorgi, F., van der Meer, T.J., Vink, A., Zonneveld, K.A.F., Vercauteren, D., Vlassenbroeck, J., Louwye, S., 2009. Process length variation in cysts of a dinoflagellate, *Lingulodinium machaerophorum*, in surface sediments and its potential use as a salinity proxy. *Marine Micropalaeontology* 70, 54–69.
- Metwalli, F.I., Ismail, A., Metwalli, M.S., El Shafei, I.M., 2023. Sequence stratigraphic evaluation for the Abu Madi Formation, Abu Madi/El Qar'a/Khilala gas fields, onshore Nile Delta, Egypt. *Petroleum Research* 8, 514–523.
- Morley, R.J., 1995. Biostratigraphic characterization of systems tracts in Tertiary sedimentary basins. *Proceedings of the International Symposium on Sequence Stratigraphy in SE Asia*, May 1995. Indonesian Petroleum Association, Jakarta, pp. 49–71.
- Nabawy, B.S., Abd El Aziz, E.A., Ramadan, M., Shehata, A.A., 2023. Implication of the micro and lithofacies types on the quality of a gas-bearing deltaic reservoir in the Nile Delta, Egypt. *Scientific Reports* 13, 8873.
- N.C.G.S. (National Committee of Geological Sciences), 1976. Miocene rock stratigraphy of Egypt. *Egyptian Journal of Geology* 18 (1), 1–69.
- Ouda, Kh., Obaidalla, N., 1995. The geologic evolution of the Nile Delta area during the Oligocene–Miocene. *Egyptian Journal of Geology* 39 (1), 77–111.
- Pearson, D.L., 1984. Pollen/spore color 'standard'. Phillips Petroleum Company Exploration Projects Section, Geological Branch. Unwin Hyman, Boston, 600 pp.
- Pellaton, C., Gorin, G.E., 2005. The Miocene New Jersey passive margin as a model for the distribution of sedimentary organic matter in siliciclastic deposits. *Journal of Sedimentary Research* 75 (6), 1011–1027.
- Popescu, S.-M., Dalesme, F., Jouannic, G., Escarguel, G., Head, M.J., Melinte-Dobrinescu, M.C., Suto-Szentai, M., Bakrac, K., Clauzon, G., Suc, J.-P., 2009. *Galeacysta etrusca* complex, dinoflagellate cyst marker of Paratethyan influxes into the Mediterranean Sea before and after the peak of the Messinian Salinity Crisis. *Palynology* 33 (2), 105–134.
- Rizzini, A., Vessani, F., Cococetta, V., Milad, G., 1978. Stratigraphy and sedimentation of Neogene–Quaternary section in the Nile Delta area. *Marine Geology* 27, 327–348.
- Roncaglia, L., Kuijpers, A., 2006. Revision of the palynofacies model of Tyson (1993) based on recent high-latitude sediments from the North Atlantic. *Facies* 52, 19–39.
- Roveri, M., Bertini, A., Cosentino, D., Di Stefano, A., Gennari, R., Gliozzi, E., Grossi, F., Iaccarino, S.M., Lugli, S., Manzi, V., Taviani, M., 2008. A high-resolution stratigraphic framework for the latest Messinian events in the Mediterranean area. *Stratigraphy* 5 (3–4), 323–342.
- Roveri, M., Flecker, R., Krijgsman, W., Lofi, J., Lugli, S., Manzi, V., Sierro, F.J., Bertini, A., Camerlenghi, A., De Lange, G., Govers, R., Hilgen, F.J., Hübscher, C., Meijer, P.Th., Stoica, M., 2014. The Messinian salinity crisis: past and future of a great challenge for marine sciences. *Marine Geology* 349, 113–125.
- Ruggieri, G., 1967. The Miocene and later evolution of the Mediterranean sea. In: Adams, C.G., Ager, D.V. (Eds.), *Aspects of Tethyan Biogeography*. Vol. 7. The Systematics Association, London, pp. 283–290.
- Said, R., 1990. Cenozoic. In: Said, R. (Ed.), *The Geology of Egypt*. A. A. Balkema, Rotterdam/Brookfield, pp. 451–486.
- Sarhan, M.A., Hemdan, K., 1994. North Nile Delta structural setting and trapping mechanism, Egypt. *Proceedings of the 12th Petroleum Conference of EGPC* 12 (1), 1–17.
- Sarhan, M.A., Collier, R., Basal, A., Abdel Aal, M.H., 2014. Late Miocene normal faulting beneath the northern Nile Delta: NNW propagation of the Gulf of Suez Rift. *Arabian Journal of Geosciences* 7, 4563–4571.
- Sestini, G., 1989. Nile Delta: a review of depositional environments and geological history. In: Whateley, M.K.G., Pickering, K.T. (Eds.), *Deltas: Sites and Traps for Fossil Fuel*. Geological Society, London, Special Publications 41, 99–127.
- Sestini, G., 1995. Egypt. In: Kulke, H. (Ed.), *Regional Petroleum Geology of the World, Part II: Africa, America, Australia and Antarctica*. Lubrecht & Cramer Ltd., Stuttgart, pp. 66–87.
- Shalaby, A., Sarhan, M.A., 2023. Pre and post Messinian deformational styles along the northern Nile Delta Basin in the framework of the Eastern Mediterranean tectonic evolution. *Marine Geophysical Research* 44, 22.
- Shebl, S., Ghorab, M., Mahmoud, A., Shazly, T., Abuhagaza, A.A., Shibl, A., 2019. Linking between sequence stratigraphy and reservoir quality of Abu Madi Formation utilizing well logging and seismic analysis at Abu Madi and El Qar'a fields, Nile Delta, Egypt. *Egyptian Journal of Petroleum* 28, 213–223.
- Soliman, A., El Atfy, H., 2024. The history of palynology in Egypt. *Palynology* 48 (2), 2273940.
- Soliman, A., Piller, W.E., Dybkjaer, K., Slimani, H., Auer, G., 2023. Middle Miocene (Serravallian; upper Badenian–lower Sarmatian) dinoflagellate cysts from Bad Deutsch Altenburg, Vienna Basin, Austria. *Palynology* 47 (1), 2116498.
- Thompson, C.L., Dembicki Jr., H., 1986. Optical characteristics of amorphous kerogens and hydrocarbon-generating potential of source rocks. *International Journal of Coal Geology* 6, 229–249.
- Traverse, A., 2007. *Paleopalynology*. Springer, Dordrecht, 813 pp.
- Tyson, R.V., 1993. Palynofacies analysis. In: Jenkins, D.J. (Ed.), *Applied Micropalaeontology*. Kluwer Academic Publishers, Dordrecht, pp. 153–191.

- Tyson, R.V., 1995. *Sedimentary Organic Matter: Organic Facies and Palynofacies*. Chapman and Hall, London, 615 pp.
- Vasiliev, I., Mezger, E.M., Lugli, S., Reichert, G., Manzi, V., Roveri, M., 2017. How dry was the Mediterranean during the Messinian salinity crisis? *Palaeogeography, Palaeoclimatology, Palaeoecology* 471, 120–133.
- Wang, X., Zhu, X., Lai, J., Lin, X., Wang, X., Du, Y., Huang, C., Zhu, Y., 2024. Paleoenvironmental reconstruction and organic matter accumulation of the Paleogene Shahejie oil shale in the Zhanhua Sag, Bohai Bay Basin, Eastern China. *Petroleum Science* 21 (3), 1552–1568.
- Wei, C., Jardine, P.E., Gosling, W.D., Hoorn, C., 2023. Is Poaceae pollen size a useful proxy in palaeoecological studies? New insights from a Poaceae pollen morphological study in the Amazon. *Review of Palaeobotany and Palynology* 308, 104790.
- Zaghloul, Z.M., Elgamal, M.M., El Araby, H., Abdel Wahab, W., 2001. Evidences of geotectonic and ground motions in the Northern Nile Delta, In: Zaghloul, Z., Elgamal, M.M. (Eds.), *Deltas: Modern and Ancient*. Mansoura University, Mansoura City, pp. 285–314.
- Zonneveld, K.A.F., Brummer, G.J.A., 2000. Ecological significance, transport and preservation of organic-walled dinoflagellate cysts in the Somali Basin, NW Arabian Sea. *Deep Sea Research II* 47, 2229–2256.
- Zonneveld, K.A.F., Versteegh, G.J.M., De Lange, G.J., 1997. Preservation of organic walled dinoflagellate cysts in different oxygen regimes: a 10,000 year natural experiment. *Marine Micropaleontology* 29, 393–405.
- Zonneveld, K.A.F., Versteegh, G.J.M., de Lange, G.J., 2001. Palaeoproductivity and post depositional aerobic organic matter decay reflected by dinoflagellate cyst assemblages of the Eastern Mediterranean S1 sapropel. *Marine Geology* 172, 181–195.
- Zonneveld, K.A.F., Bockelmann, F., Holzwarth, U., 2007. Selective preservation of organic walled dinoflagellate cysts as a tool to quantify past net primary production and bottom water oxygen concentrations. *Marine Geology* 237, 109–126.
- Zonneveld, K.A.F., Chen, L., Möbius, J., Mahmoud, M.S., 2009. Environmental significance of dinoflagellate cysts from the proximal part of the Po-river discharge plume (off southern Italy, Eastern Mediterranean). *Journal of Sea Research* 62, 189–213.
- Zonneveld, K.A., Marret, F., Versteegh, G.J., Bogus, K., Bonnet, S., Bouimetarhan, I., Crouch, E., de Vernal, A., Elshanawany, R., Edwards, L., Esper, O., Forke, S., Grøsfjeld, K., Henry, M., Holzwarth, U., Kieft, J.-F., Kim, S.-Y., Ladouceur, S., Ledu, D., Chen, L., Limoges, A., Londeix, L., Lu, S.-H., Mahmoud, M.S., Marino, G., Matsouka, K., Matthiessen, J., Mildenhall, C., Mudie, P., Neil, L., Pospelova, V., Qi, Y., Radi, T., Richerol, T., Rochon, A., Sangiorgi, F., Solignac, S., Turon, J.-L., Verleye, T., Wang, Y., Wang, Z., Young, M., 2013. Atlas of modern dinoflagellate cyst distribution based on 2405 datapoints. *Review of Palaeobotany and Palynology* 191, 1–197.